

Spring 4-2018

Multi-Scale Fluid Flow Analysis of the Cardiovascular System

Zaid Mahmood
Embry-Riddle Aeronautical University

Follow this and additional works at: <https://commons.erau.edu/edt>



Part of the [Biomechanical Engineering Commons](#), and the [Medical Physiology Commons](#)

Scholarly Commons Citation

Mahmood, Zaid, "Multi-Scale Fluid Flow Analysis of the Cardiovascular System" (2018). *Doctoral Dissertations and Master's Theses*. 394.

<https://commons.erau.edu/edt/394>

This Thesis - Open Access is brought to you for free and open access by Scholarly Commons. It has been accepted for inclusion in Doctoral Dissertations and Master's Theses by an authorized administrator of Scholarly Commons. For more information, please contact commons@erau.edu.

MULTI-SCALE FLUID FLOW ANALYSIS OF THE CARDIOVASCULAR SYSTEM

by

Zaid Mahmood

A Thesis Submitted to the College of Engineering Department of Mechanical
Engineering in Partial Fulfillment of the Requirements for the Degree of
Master of Science in Mechanical Engineering

Embry-Riddle Aeronautical University
Daytona Beach, Florida
April - 2018

MULTI-SCALE FLUID FLOW ANALYSIS OF THE CARDIOVASCULAR SYSTEM

by

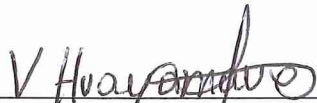
Zaid Mahmood

This thesis was prepared under the direction of the candidate's Thesis Committee Chair, Dr. Eduardo Divo, Daytona Beach Campus, and Thesis Committee Members Dr. Victor Huayamave, Daytona Beach Campus, and Dr. Marcus Ni, Daytona Beach Campus, and has been approved by the Thesis Committee. It was submitted to the Department of Mechanical Engineering in partial fulfillment of the requirements for the degree of Master of Science in Mechanical Engineering

Thesis Review Committee:



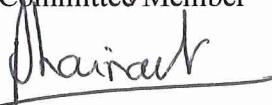
Eduardo Divo, Ph.D.
Committee Chair



Victor Huayamave, Ph.D.
Committee Member



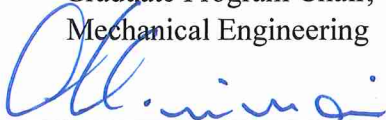
Marcus Ni, Ph.D.
Committee Member



Jean-Michel Dhainaut, Ph.D.
Graduate Program Chair,
Mechanical Engineering



Eduardo Divo, Ph.D.
Department Chair,
Mechanical Engineering



Maj Mirmirani, Ph.D.
Dean, College of Engineering



Christopher Grant, Ph.D.
Associate Vice President of Academics

4/25/2018
Date

Acknowledgements

I would like to express my appreciation to the Department of Mechanical Engineering, mainly Professor Eduardo Divo for his advice and endless support. Professor Divo has been one of the most inspirational people in my life. He never hesitated to help me whenever I have a question about my research. I would also like to thank Professor Alain Kassab and Dr. William Decampli for their support and guidance to help me with progressing this work.

I would also like to say thank you very much for all of my professors in the Department of Mechanical Engineering for their advice and support regarding my research. Without those folks, my journey to pursuing my masters in mechanical engineering would have been difficult.

My gratitude also goes to my parents for their unconditional support and love through all this long process. They always believe in me and support me to achieve my goals. My friends here in the United States of America and there back home in Iraq, I would like to say thanks for your support as well.

Abstract

Researcher: Zaid Mahmood
Title: Multi-Scale Fluid Flow Analysis of the Cardiovascular System
Institution: Embry-Riddle Aeronautical University
Degree: Master of Science in Mechanical Engineering
Year: 2018

The hypoplastic left heart syndrome (HLHS) is one of the rarest congenital heart diseases affecting infants. Out of 150 babies born, one baby suffers from congenital heart disease. Furthermore, nine percent out of those suffering from congenital heart disease specifically suffer from hypoplastic left heart syndrome (HLHS). To this end, the Fontan operation which is a procedure to generate a harmonic blood flow in single functioning ventricle patients has been executed to palliate HLHS patients. In this operation, the inferior vena cava (IVC) and the superior vena cava (SVC), carrying the low-oxygenated blood returning from the lower and upper body back to the heart, are connected to the pulmonary arteries. Despite the fact that the Fontan operation has been executed for years, it is still not the effective palliation to heal HLHS patients since those who have undergone this procedure experience chronic diseases. In order to mitigate the risk associated with the Fontan procedure, an Injection Jet Shunt (IJS) is suggested to connect the aorta to the total cavopulmonary connection (TCPC). Thus, the purpose of utilizing the IJS is to add momentum to the pulmonary arteries. This research is concerning two models, baseline model and IJS model. Those two models represent a simplified Fontan physiology. The purpose of this research is to distinguish the effectiveness of using the IJS.

Table of Contents

	Page
Thesis Review Committee.....	i
Acknowledgements.....	ii
Abstract.....	iii
List of Figures.....	vi
List of Tables.....	vii

Chapter

I	Introduction.....	1
	Background.....	1
	Research Significance.....	2
	Research Objective.....	2
	Research Approach.....	3
	Research Layout.....	3
II	Review of the Relevant Literature.....	5
	Heart Physiology.....	5
	Hypoplastic Left Heart Syndrome.....	6
	Norwood Procedure.....	7
	Bidirectional Glenn Procedure.....	8

	Fontan Procedure	10
III	Methodology	12
	Baseline Model	12
	Injection Jet Shunt (IJS)	14
	Lumped Parameter Model	16
	Lumped Parameter Model (LPM) Coupled to the Computational Fluid Dynamics (CFD)	22
	CFD Solver and Fluid Domain Meshing	24
IV	Results and Discussion	25
V	Conclusion – Limitation – Future Work	32
	References	33
	Appendices	36
	Appendix 1: Abbreviations Resulted from the Equations	36
	Appendix 2: The Fontan Procedure Model Parameters	37
	Appendix 3: Modeling Instructions	38
	Appendix 4: CFD-LPM Coupling Charts-Baseline Model	46
	Appendix 5: CFD-LPM Coupling Charts-IJS Model	51
	Appendix 6: LPM Pressure & Flow Charts - Baseline Model	57
	Appendix 7: LPM Pressure & Flow Charts - IJS Model	58

List of Figures

	Page
Figure	
Figure 1: Hypoplastic Left Heart Syndrome.....	1
Figure 2: The Cardiovascular System.....	5
Figure 3: Norwood Procedure.....	8
Figure 4: Bidirectional Glenn Procedure	9
Figure 5: The Stages of Fontan Procedure.....	11
Figure 6: Baseline Model.....	13
Figure 7: Injection Jet Shunt.....	15
Figure 8: Lumped Parameter Model	16
Figure 9: Elastance of the right ventricle.....	19
Figure 10: Lumped Parameter Model with IJS.....	21
Figure 11: Coupling Process.....	23
Figure 12: CFD-LPM Coupling Process.....	23
Figure 13: The Baseline Model Pressure	26
Figure 14: Velocity Field of the Baseline Model.....	27
Figure 15: The IJS Model Pressure	28
Figure 16: Velocity Field of the IJS Model	29

List of Tables

	Page
Table	
Table 1: Flow Values in the Baseline & IJS Models.....	30
Table 2: Pressure Values in the Baseline & IJS Models.....	31

Chapter I

Introduction

Background

Infants who are born with a single functioning heart ventricle go through a sequence of surgical operations to attain the best possible cardiac output out of the single functioning heart ventricle. This issue is related to hypoplastic left heart syndrome (HLHS) [1] [2]. The hypoplastic left heart syndrome (HLHS) is a scarce congenital heart disease. This syndrome means the left heart is severely underdeveloped. The left heart consists of the left ventricle, the mitral valve, the aortic valve, and the ascending part of the aorta. In general, this syndrome may cause some undefeated issues to the patients. Single ventricle issue is one of the many congenital cardiac disorders. 50% of patients reaching the age of 20 face a death risk since the right ventricle is not pumping the blood efficiently [3]. Figure (1) below displays how the left heart is underdeveloped.

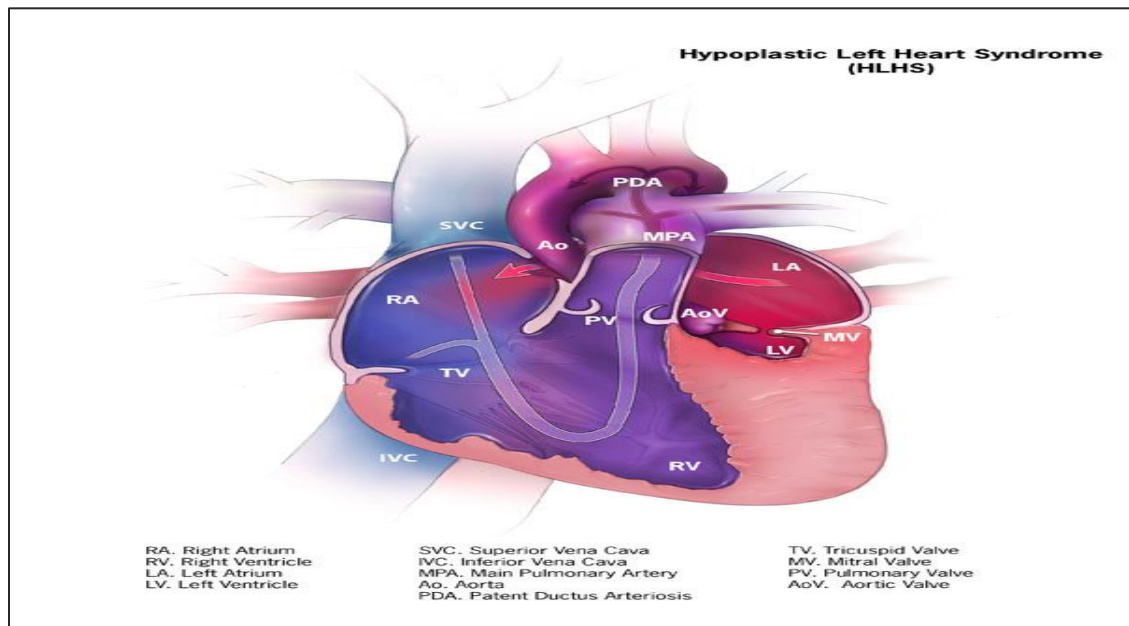


Figure 1: Hypoplastic Left Heart Syndrome [4]

The main variance in the human cardiovascular anatomy for the normal human heart and the unhealthy heart suffering from HLHS is palliative procedures that are performed in the following three consecutive stages. The first stage is called Norwood procedure. In this stage, the hypoplastic aorta is rejoined to the right ventricle rather than link it to the pulmonary root. Furthermore, the second stage concerning the Glenn procedure, the superior vena cava (SVC) is separated from the right atrium and linked straight to the right pulmonary artery. Finally, the last stage is named as Fontan procedure. The inferior vena cava (IVC) is separated from the right atrium and connected straight to the pulmonary arteries. This procedure produces a total cavopulmonary connection [5].

Research Significance

This research concentrates on patients suffering from a single ventricle heart disease (HLHS). As mentioned earlier in this research, there are three consecutive stages that need to be followed in order to improve the cardiovascular system. This research is focusing practically on the third stage which is the Fontan surgery. This study helps comprehend the advantage of adding the injection jet shunt (IJS) to the original procedure. The role of the injection jet shunt is to link the ascending aorta to the total cavopulmonary connection (TCPC).

Research Objective

The objective of this study is to validate the utilization of the injection jet shunt in the Fontan procedure by relying on a commercial software called Star-CCM+ as well as Catia V5 used to build the geometry.

Research Approach

To complete the research objective, the following steps will be conducted as follow:

- a. Step1- Literature review: previous comprehensive studies about the Fontan procedure
- b. Step 2- building the baseline model as well as the IJS model by using Catia V5 to assist the CFD analysis in Star CCM+ software.
- c. Step3- Comparison Analysis: comparing the results between the baseline model and the aftermath of adding the IJS to the baseline model.
- d. Step4: Procedure improvement: based on the results provided, the importance of the IJS is being explained, and the cardiac output will be enhanced.

Research Layout

This research will be presented in five chapters. The summary of each chapter will be addressed as follow:

- a. Chapter one- Introduction: a brief description of the importance of this study in the medical and engineering fields will be summarized in this chapter.
- b. Chapter two – Literature Review: This chapter offers a complete review of previous research that has been done in the medical and engineering fields.
- c. Chapter three - Methodology: a detailed illustration about conducting two models by using the CFD analysis.
- d. Chapter four – Results and Discussions: the results obtained from the CFD analysis will be discussed and demonstrated in this chapter.

- e. Chapter Five – Conclusion, limitation, and future work: the main findings derived from this study will be presented, also, several recommendations will be suggested for further research work.

Chapter II

Review of the Relevant Literature

Heart Physiology

The cardiovascular system contains the heart, a unique organ of the human body, placed in the middle of the body and the vessels of the body that help convey the blood. This system provides oxygen, obtained from the air through the lungs, to the organs throughout the body. It is also responsible for the deletion of the waste in the body. The blood circulation is also responsible for moving nutrients like amino acids, and others. [6] [7]. Furthermore, the heart consists of two sides, the left and right side. The right side of the heart is in charge of pumping the blood to the lungs, and it works by receiving the poor-oxygenated blood through veins to the right ventricle, and then through the tricuspid valve to the lungs to get oxygenated. While the left side of heart is responsible for pushing the blood to the rest of the body. It starts when the left atrium receives the red blood through the mitral valve [8]. Figure (2) below shows the cardiovascular system.

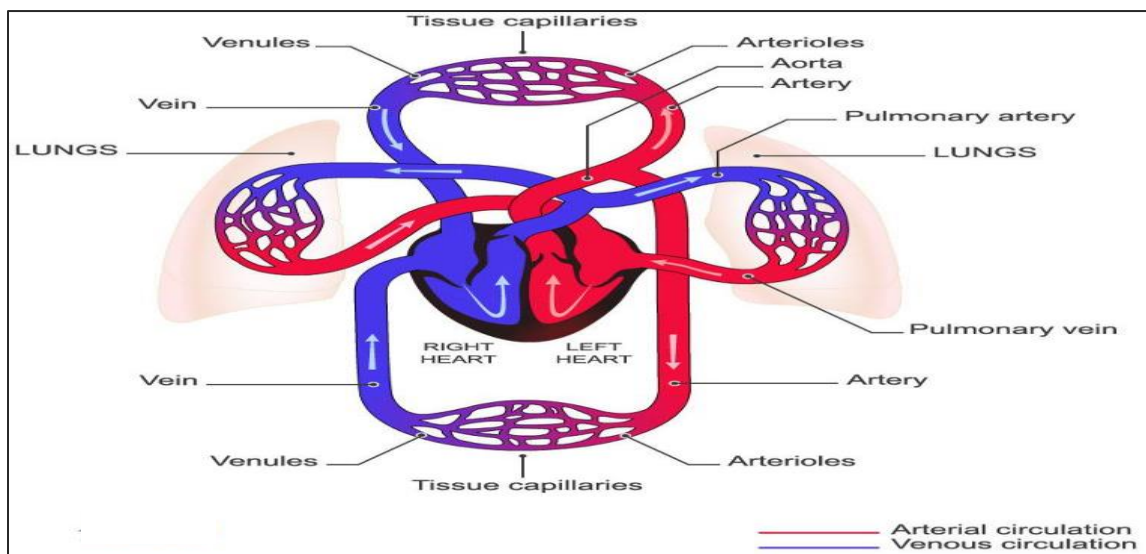


Figure 2: The cardiovascular system [9]

Hypoplastic Left Heart Syndrome

Many patients around the globe have a congenital heart disease (CHD), the most common reason of a major congenital abnormality, demonstrating key universal health difficulties. Twenty-eight percent of all main congenital abnormalities involve heart failings [10]. One of the rarest problems occurs to the infants is the hypoplastic left heart syndrome (HLHS) that distresses normal blood flow through the heart.

This happens when infants grow through pregnancy, the left side of the heart does not form properly [11]. The reasons why the left side of the heart is not performing properly is because mitral valve, left ventricle, aortic valve, and the ascending portion of the aorta are severely underdeveloped. Usually, an infant with hypoplastic left heart syndrome (HLHS), the left side of the heart cannot pump blood to the other organs efficiently. In situations similar to that, the right side of the heart will be responsible for pumping the blood to the whole body [12].

The hypoplastic left heart syndrome (HLHS) embodies fully nine percent of those with congenital heart disease (CHD). If infants being left without medical treatment, the defect is nearly without doubt lethal [13]. In general, there is no gene is directly associated to the hypoplastic left heart syndrome (HLHS). But, many genetic relations have been recognized without any reliable marker [14]. Even though lethal if left untouched, this defect is exceedingly curable with reconstructive surgical procedures that will be addressed in this research.

Norwood Procedure

The Norwood procedure was presented as the first stage surgical procedure for infants with hypoplastic left heart syndrome (HLHS). It has later been applied to many cardiac flaws determined by the existence of a practical single ventricle with complete outflow tract block [15].

This procedure is performed right after the birth [14]. Many of the infants leave the hospital between ten days to two weeks after the end of the Norwood operation. The procedure works when the right ventricle is linked to a rebuilt aorta with the use of the near core pulmonary artery for the systemic outflow. A shunt from the pulmonary artery to the systemic circulation helps regenerating the pulmonary blood flow [16].

The Norwood procedure tries to avoid cardiopulmonary bypass and contains of a stent of the ductus arteriosus, balloon atrial septostomy, and a branch pulmonary artery banding.

The less disturbing environment of the Norwood procedure and deferral of the danger of a main open-heart operation to an older age are meant to help improve survival, neurologic, and cardiac practical outcomes. Latest reports of survival after the Norwood procedure are as good as with those achieved with the conventional surgical Norwood. Furthermore, the Norwood procedure has turned out to be the favored first operation for HLHS mitigation [17].

The expansion of Norwood stage mitigation significantly enhanced the outcome of the newborns with HLHS. Conversely, with the substantial development in surgical operation, this procedure is a practical experiment and still holds major mortality and sickness [18]. Below, figure (3) displays the Norwood procedure.

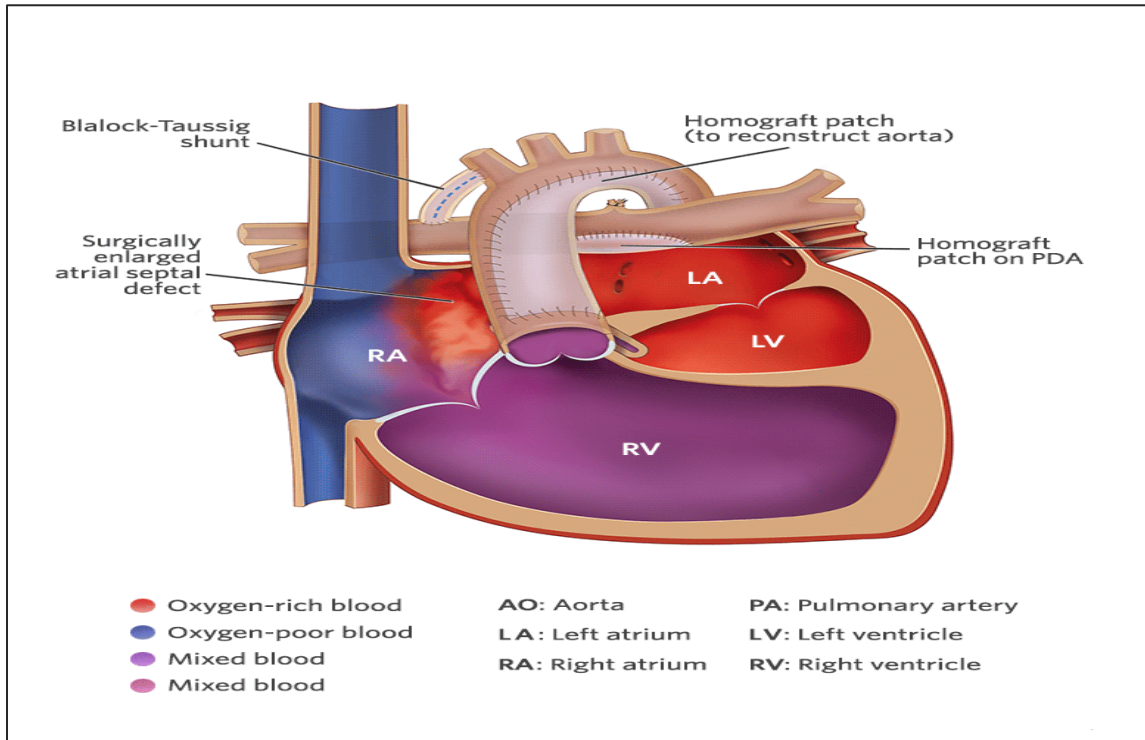


Figure 3: Norwood Procedure [19]

Bidirectional Glenn Procedure

The bidirectional Glenn procedure (BDG) that is also called the hemi-Fontan (HF) operation is the second stage in the process to a crucial Fontan mitigation. Even though the bidirectional Glenn procedure (BDG) is predominant in the Western world, it has faced limited utilization in the evolving world [20]. This procedure is executed at six to eight

months of babies' age [14]. The perfect age to implement the bidirectional Glenn procedure (BDG), however, stays indeterminate [21].

The bidirectional Glenn procedure (BDG) helps involve connection of the superior vena cava to the pulmonary artery [6]. It also assists enhancing the efficiency of gas exchange without concerning about volume or pressure overload of the ventricle contrasting the pulmonary trunk band or systemic-pulmonary arterial shunt. After the bidirectional Glenn procedure (BDG) is done, the medical definition of the idea of total cavopulmonary connection (TCPC) has been started [6]. Even though it enhances overall survival, there is a number of babies who might be at a credible hazard [20]. Typically, the bidirectional Glenn procedure (BDG) is a valuable intermediate comforting operation prior to the Fontan operation. Figure (4) shows the Bidirectional Glenn procedure.

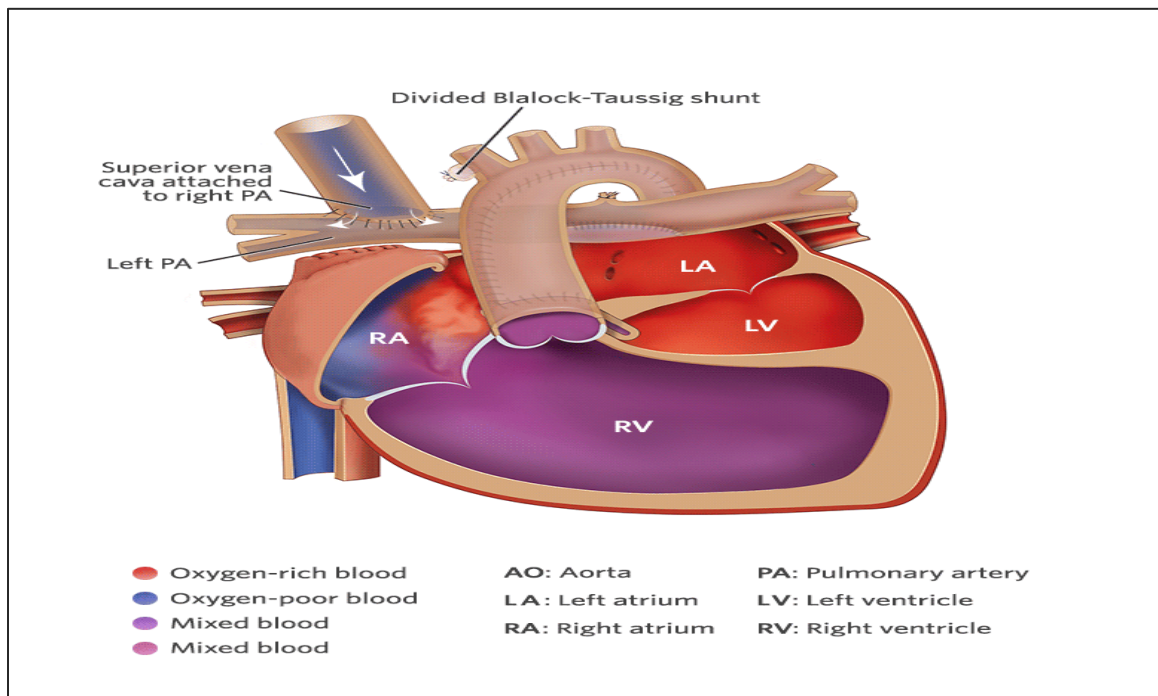


Figure 4: Bidirectional Glenn procedure [22]

Fontan Procedure

The Fontan procedure is the last palliative operation for patients with hypoplastic left heart syndrome (HLHS) [23]. It was established in 1971 by a cardiac surgeon, Francis Fontan [24] [25]. Usually, the procedure is performed to patients by the age of eighteen months to five years (most often near 4 years) [14].

The Fontan procedure has experienced several consecutive practical alterations. To illustrate, early alterations of this procedure linked the pulmonary arteries to the right atrium. Several approaches such as valve conduits, patches, and others were utilized. Initially, it was assumed that the right atrium would enhance the pulmonary blood flow. Conversely, de Leval found after conducting a number of experiments that the right atrium expanded, then the contractile function was weakened which caused an energy lack and essentially reduced pulmonary blood flow. Even though lots of efforts put to develop this technique, it is still considered obsolete [26].

The second technique of the Fontan procedure was consequently enhanced to the lateral tunnel approach (LT). In this approach, the lateral tunnel Fontan utilizes a baffle within the right atrium (RA) and the superior vena cava (SVC) is stitched straight to the right pulmonary artery (RPA) [27].

The latest technique is the extra-cardiac conduit (EC). The extra-cardiac Fontan operates an outer conduit to link the inferior vena cava (IVC) into the pulmonary arteries [27]. The Fontan is achieved in order to make poor-oxygenated blood coming back from the body go to the lungs. Figure (5) shows the stages of developing Fontan operation.

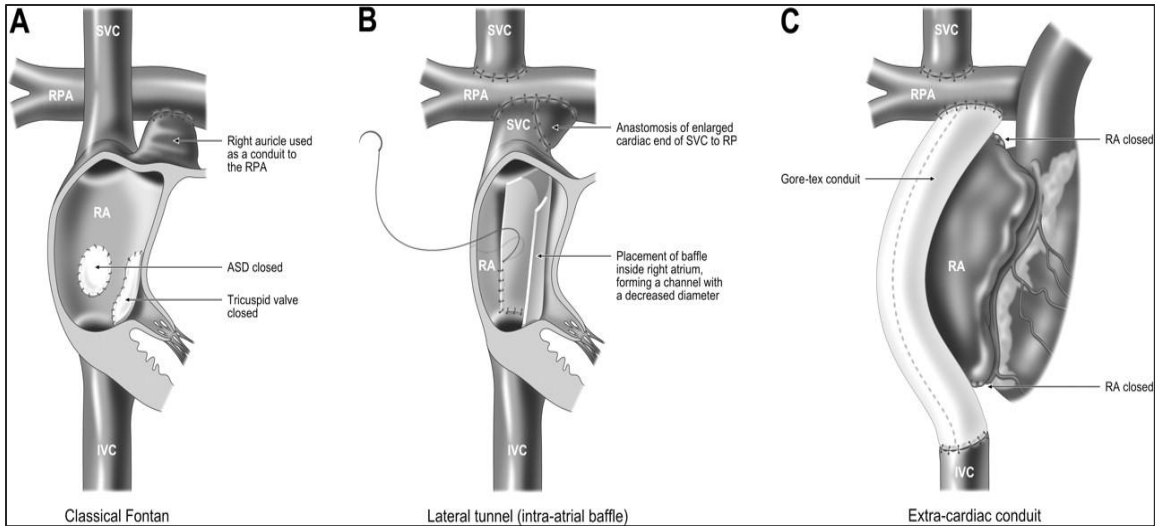


Figure 5: The stages of Fontan procedure [28]

Although, the Fontan procedure has many benefits toward patients with hypoplastic left heart syndrome (HLHS), it is still characterized by low cardiac output that is less reactive to normal physical stressors [29], high venous pressure, high pulmonary vascular resistance, and partially low arterial oxygen saturation [23]. Most likely, patients with a single ventricle who have undergone the Fontan procedure have liver disease (LD) [30]. Roughly, twenty one percent of patients who have gone through this procedure could have cirrhosis. Also, patients face numerous late obstacles such as heart failure, arrhythmia, and hepatic dysfunction [30].

Chapter III

Methodology

Baseline Model

The 3D CAD model, representing a synthetic geometry of the cardiovascular system, was built by Catia V5. This model can be classified into five main parts which are:

- A. Aortic artery which is the major artery of the body responsible for supplying rich-oxygenated blood to the systemic circulations.
- B. Superior vena cava which is a large vein carrying blood through the upper systemic circulation
- C. Inferior vena cava which is a large vein responsible for carrying the blood in the lower systemic circulation back to the pulmonary arteries.
- D. Left and right pulmonary arteries which are carrying the blood coming from the systemic circulations back to the right atrium.
- E. Total cavopulmonary connection which is the Fontan procedure part representing where the systemic circulations and the pulmonary arteries connect.

The length of each part does not mimic what the real human's cardiovascular system has since the blood journey through the body is too long and complicated. However, the diameters of each part were taken from Fontan patients who are by the age of 2 - 4 years old. The diameters of the aorta, inferior vena cava, superior vena cava, and pulmonary arteries are 18 mm, 18 mm, 12mm, and 9 mm consecutively [31]. Figure (6) below displays the synthetic CAD model.

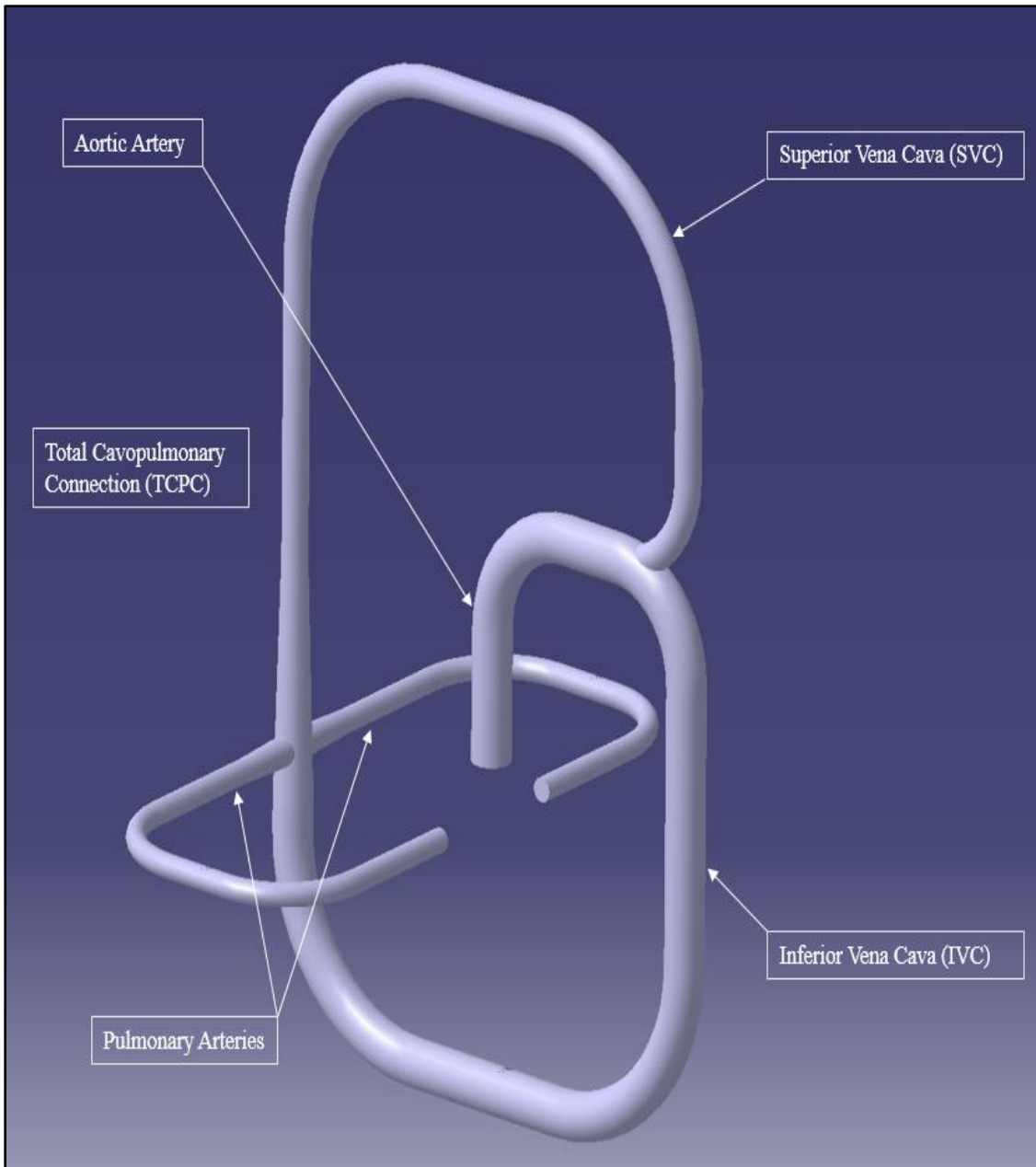


Figure 6: Baseline Model

Injection Jet Shunt (IJS)

The research mainly focuses on the addition of the graft known as Injection Jet Shunt (IJS) to the Fontan procedure. The Injection Jet Shunt (IJS) basically connects the aorta to the pulmonary arteries. This graft was modeled by Catia V5 in such a way to raise the flow in the pulmonary arteries by utilizing the mechanical energy obtained from the heart itself. The main determination of using the Injection Jet Shunt (IJS) is not only increasing the flow in the pulmonary arteries but also improving the blood circulation through the body, contributing in a better oxygen delivery, reducing the inferior vena cava pressure, and decreasing the loss of energy by adding pulse pressure to the pulmonary arteries.

The IJS is modeled with 3mm nozzles. This IJS model will be investigated and compared to the baseline model. This research will assist considering the use of the IJS connected to the Fontan procedure. Figure (7) below displays the Injection Jet Shunt of 3mm diameter.

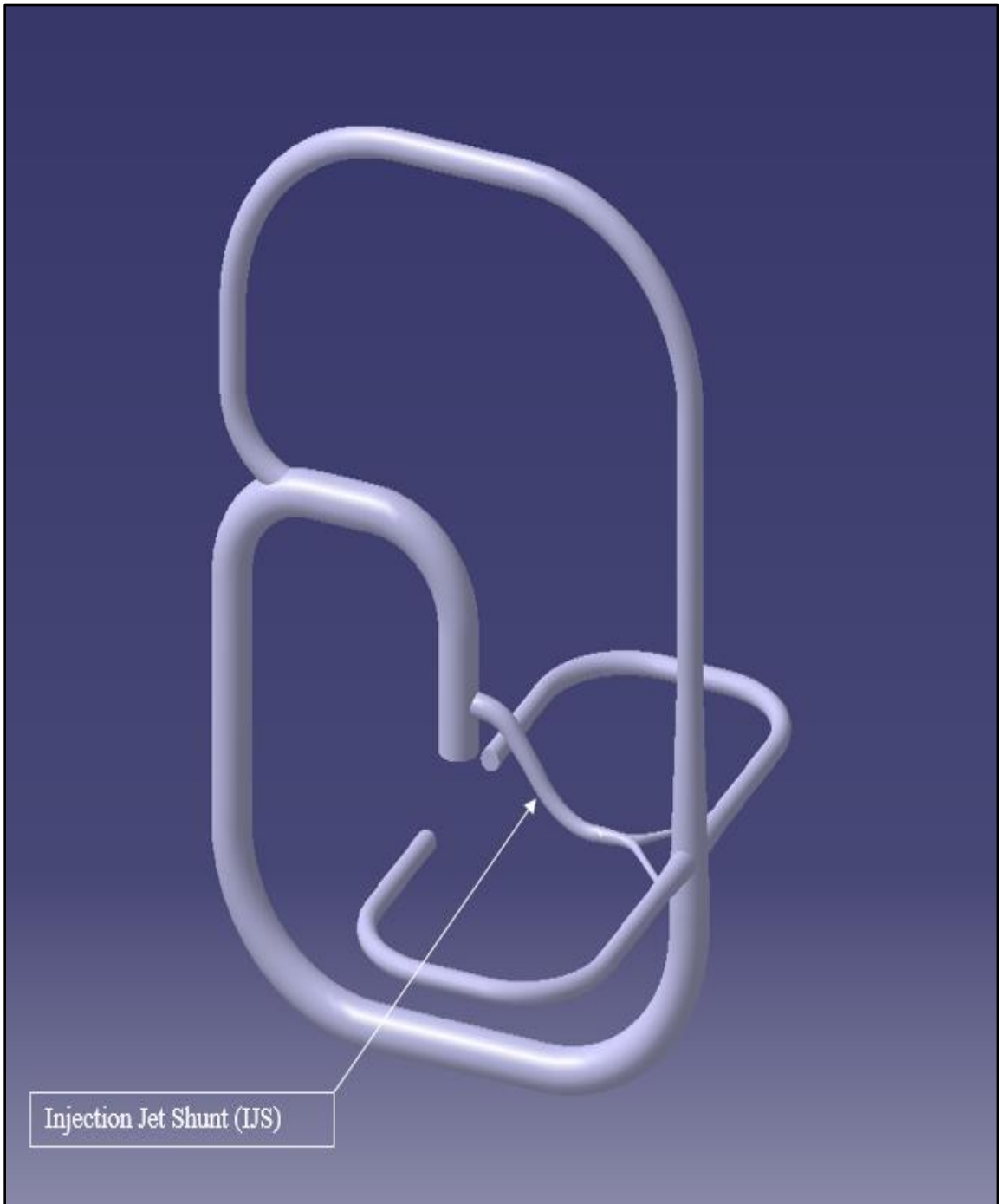


Figure 7: Injection Jet Shunt

The basic concept of understanding the blood flow is basically accounted for the pressure difference at the inlet and outlet of each blood vessel. The blood vessels resist the blood flow passing through them, and that creates the resistance due to the friction between the blood flow and the stationary walls of the vessels. Once the pressure difference and the resistance exist, the blood flow can be easily represented by:

$$Flow = \frac{\text{pressure difference}}{\text{resistance}} \quad \text{or} \quad Q = \frac{dP}{R} \dots\dots\dots(1)$$

Where Q = blood flow (ml/s)

dP = pressure difference (mmHg)

R = resistance (mmHg - s/ ml)

The blood vessels are compliant to the flow passing through them. This can be described as follow:

$$Q = C * \frac{dP}{dt} \dots\dots\dots(2)$$

$$C = \frac{dV}{dP} \dots\dots\dots(3)$$

Where C = Compliance coefficient (ml/mmHg)

dt = time step (s)

dV = change in volume (mm³)

While the inertia of the blood flow is represented by:

$$dP = L \frac{dQ}{dt} \dots\dots\dots(4)$$

Where dQ = flow change (ml/s)

L= Inertial flow coefficient (mmhg- s²/ ml)

These differential equations have been arranged into a system of (12 DOF) in order to calculate the pressure and the flow in the blood vessels. The Fontan procedure has five lumped models which are the right heart, the upper systemic circulation, the lower systemic circulation, the left pulmonary artery, and the right pulmonary artery. In order to control the flow passing in one direction, a diode has been utilized in such a way representing heart valves, making the flow not come back to the heart.

The valve is formulated by a combination of poiseuille's Law and the Heaviside function:

$$Q(t) = \left[\frac{dP}{R_{valve}} \right] * H(dP) \dots \dots \dots (5)$$

Where H= Heaviside function

The right ventricle elastance can be utilized to simulate the time varying compliance of the right ventricle. It can be measured by knowing the maximum elastance, minimum elastance, and Double Hill function. The time varying compliance is the inverse of the right ventricle elastance.

$$E(t) = \left((E_{max} - E_{min}) * E_n(tn) \right) - E_{min} \dots \dots \dots (6)$$

The Double Hill function can be found by:

$$E_n(t) = 1.55 * \left[\frac{\left(\frac{tn}{0.7}\right)^{1.9}}{1 + \left(\frac{tn}{0.7}\right)^{1.9}} \right] * \left[\frac{1}{1 + \left(\frac{tn}{1.17}\right)^{21.9}} \right] \dots \dots \dots (7)$$

The normalized time-scale (tn) is defined by:

$$tn = \frac{t}{T_{max}} \dots \dots \dots (8)$$

The shifted heart cycle period is obtained by:

$$T_{max} = 0.2 + 0.15 * tc \dots\dots\dots(9)$$

The actual heart cycle period is defined as:

$$tc = \frac{60}{HR} \dots\dots\dots(10)$$

Where HR = heart rate

After calculating the right ventricle elastance, the time varying compliance is obtainable, and can be used in the system of differential equations.

$$C_{rv}(t) = \frac{1}{E(t)} \dots\dots\dots(11)$$

Figure (9) displays the elastance of the right ventricle with the heart rate of 120 beats / se cond.

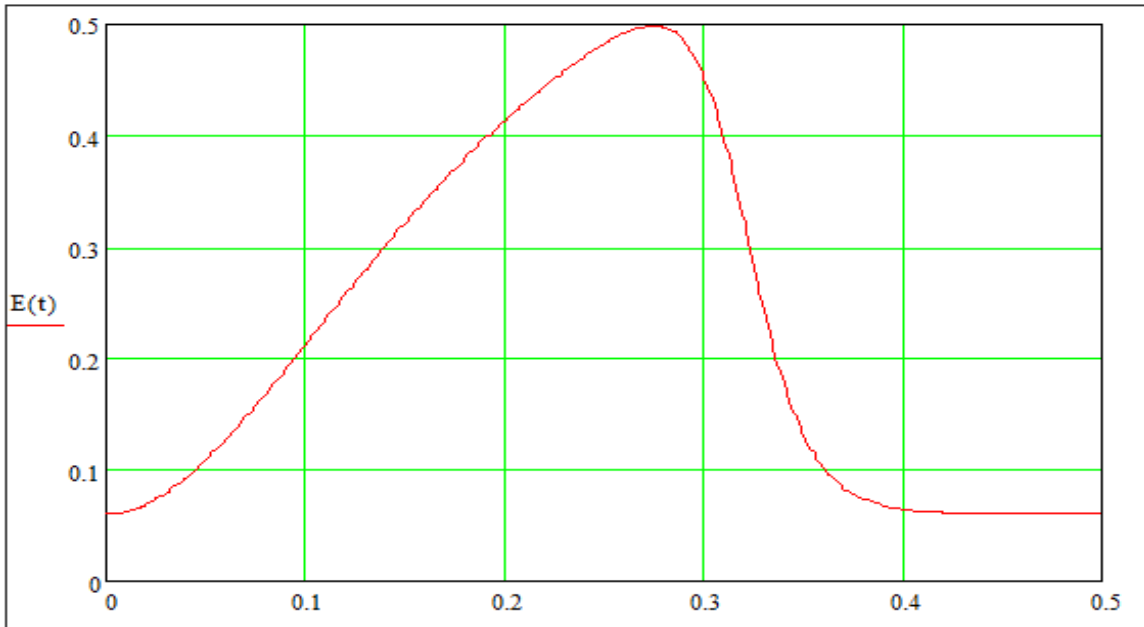


Figure 9: Elastance of the right ventricle

Since the lumped parameter model of the Fontan procedure mimics Ohm's law, Kirchhoff's Current Law (KCL) and Kirchhoff's Voltage Law (KVL) have been used to formulate the differential equations.

The system of ordinary differential equations is set as follow:

$$\frac{dp_{ra}(t)}{dt} = \frac{p_{lpc}(t) - p_{ra}(t)}{R_{lpv} * C_{ra}} + \frac{p_{rpc}(t) - p_{ra}(t)}{R_{rpv} * C_{ra}} + \frac{p_{ra}(t) - p_{rv}(t)}{R_{tv} * C_{ra}} * H(p_{ra}(t) - p_{rv}(t)) \dots \dots \dots (12)$$

$$\frac{dp_{rv}(t)}{dt} = \frac{-d C_{rv}(t)}{C_{rv} * dt} * p_{rv}(t) + \frac{p_{ra}(t) - p_{rv}(t)}{R_{tv} * C_{ra}} * H(p_{ra}(t) - p_{rv}(t)) - \frac{p_{rv}(t) - p_{rao}(t)}{R_{tv} * C_{ra}} * H(p_{rv}(t) - p_{rao}(t)) \dots \dots \dots (13)$$

$$\frac{dp_{ao}(t)}{dt} = \frac{p_{rv}(t) - p_{ao}(t)}{R_{tv} * C_{ra}} * H(p_{rv}(t) - p_{ao}(t)) - \frac{Q_{sca}(t)}{C_{ao}} - \frac{Q_{sca}(t)}{C_{ao}} \dots \dots \dots (14)$$

$$\frac{dQ_{sca}(t)}{dt} = \frac{p_{ao}(t)}{L_{sca}} - \frac{p_{sc}(t)}{L_{sca}} - \frac{R_{sca} * Q_{sca}(t)}{L_{sca}} \dots \dots \dots (15)$$

$$\frac{dp_{sc}(t)}{dt} = \frac{Q_{sca}(t)}{C_{sc}} - \frac{p_{sc}(t) - P_j(t)}{R_{svc} * C_{sc}} \dots \dots \dots (16)$$

$$\frac{dQ_{ica}(t)}{dt} = \frac{p_{ao}(t)}{L_{ica}} - \frac{p_{ic}(t)}{L_{ica}} - \frac{R_{ica} * Q_{ica}(t)}{L_{ica}} \dots \dots \dots (17)$$

$$\frac{dp_{ic}(t)}{dt} = \frac{Q_{ica}(t)}{C_{ic}} - \frac{p_{ic}(t) - P_j(t)}{R_{ivc} * C_{sc}} \dots \dots \dots (18)$$

$$\frac{dQ_{lpa}(t)}{dt} = \frac{p_j(t)}{L_{lpa}} - \frac{p_{lpc}(t)}{L_{lpa}} - \frac{R_{lpa} * Q_{lpa}(t)}{L_{lpa}} \dots \dots \dots (19)$$

$$\frac{dp_{lpc}(t)}{dt} = \frac{Q_{lpa}(t)}{C_{lpc}} - \frac{p_{lpc}(t) - p_{ra}(t)}{R_{lpv} * C_{lpc}} \dots \dots \dots (20)$$

As mentioned previously, the system of differential equations is solved by Runge-Kutta 4th order solver. This system has to have initial values. If not, the solution will be trivial.

Lumped Parameter Model (LPM) Coupled to the Computational Fluid Dynamics (CFD)

The system of equations governing the Fontan procedure analysis is set to provide the blood pressure and the blood flow in the right ventricle, superior vena cava, inferior vena cava, right pulmonary artery, and the left pulmonary artery. These blood pressure and blood flow data have been utilized as boundary conditions to simulate a transient analysis of the Fontan procedure by the commercial software known as Star CCM+ which is a computational fluid dynamics (CFD) solver established by CD-Adapco [32].

Computational fluid dynamics analysis would give an adequate knowledge about the physiology of the Fontan operation. This will help understand the blood pressure and the blood flow attributes all over the Fontan model as well as adding the Injection Jet Shunt (IJS) to the baseline model. After the Fontan procedure is being simulated, the CFD will provide new pressure and flow data. These data have been coupled to the Lumped Parameter Model (LPM) to provide time averaged solution that provides new pressure and flow curves used in the new boundary conditions to simulate the Fontan operation again. This process is being repeated consecutively so that the residuals will be decreased to the minimal level.

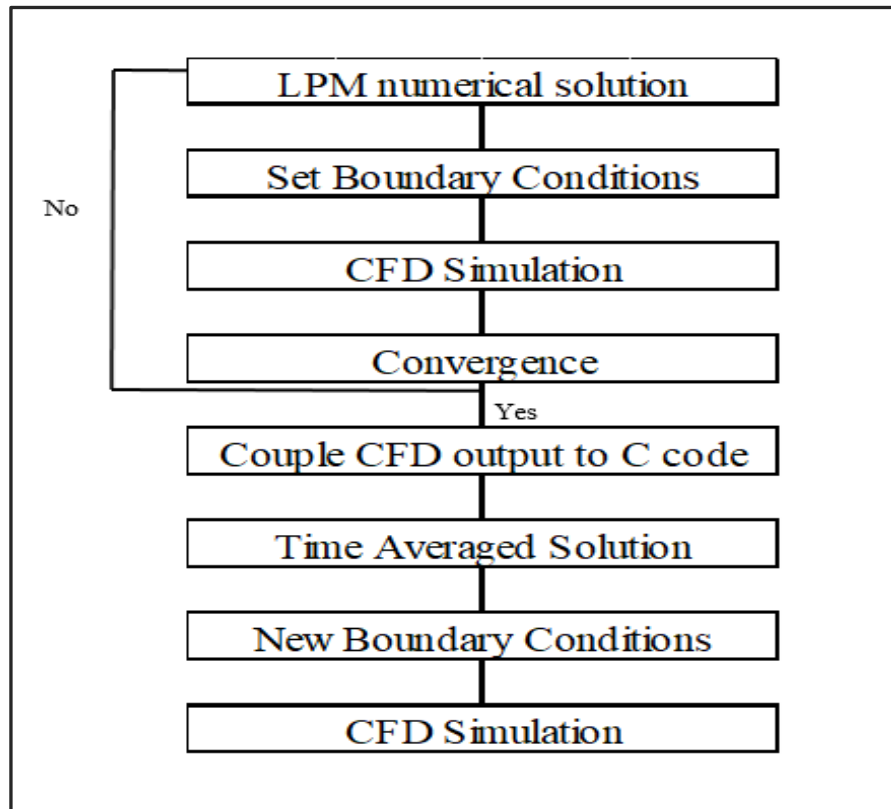


Figure 11: Coupling process

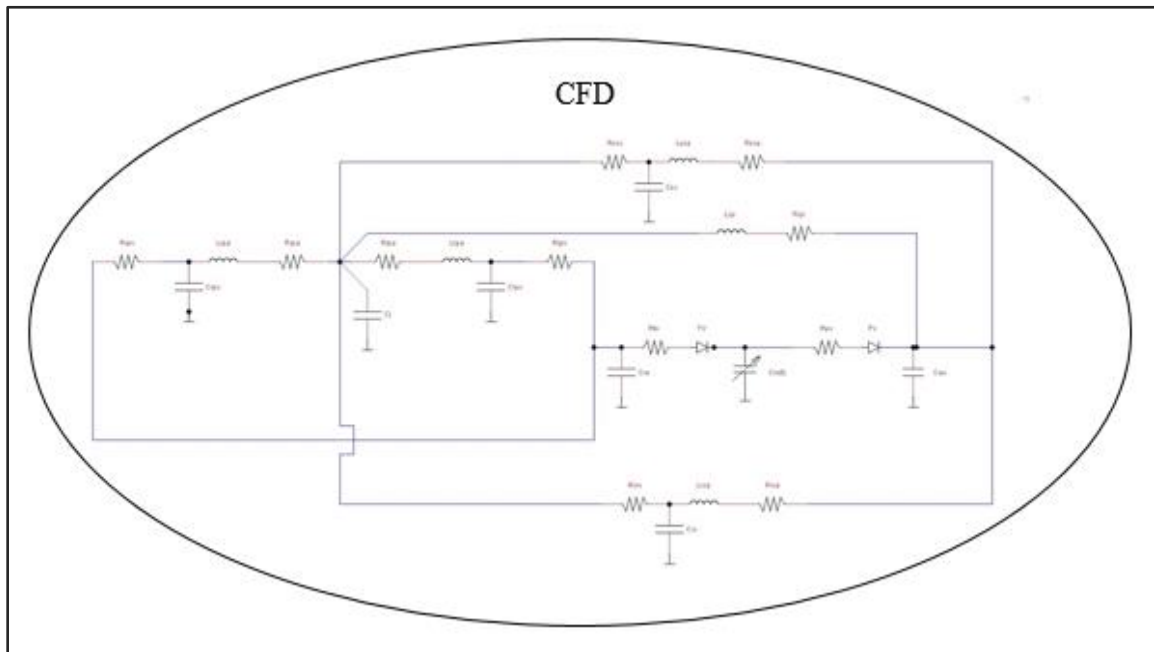


Figure 12: CFD-LPM coupling process

CFD Solver and Fluid Domain Meshing

The 3D CAD model was built by CATIA V5 as described previously. The model is imported to the CFD solver to start setting the physical parameters in the CFD setup of the Fontan operation. The CAD repair tool was used to fix any inconsistency that the model might have. The CAD repair is necessary to avoid any complications that might happen while meshing the model. Afterwards, the mesh, the discretized illustration of the computational volume that the solvers utilize to deliver a numerical solution, was generated by the Star CCM+ meshing tool. Surface remesher with the polyhedral volume, thin, prism layer mesher models were chosen as well as the automatic surface repair. Automatic surface repair was enabled to improve and optimize the mesh quality which could affect the numerical solution if it is not precise enough. The cell size of the baseline model and the IJS model was set to 3 mm with a total number of cells of 293,010 and 349,619 respectively. Furthermore, the physics that describe the Fontan procedure were set properly. The fluid domain that was set up for such a case is an incompressible Newtonian's flow with viscosity material properties and blood density. The flow field solution is governed by the Navier-Stokes equations of mass and momentum.

$$\nabla \cdot \bar{V} = 0 \dots\dots\dots(25)$$

$$\rho \frac{d\bar{V}}{dt} + \rho (\nabla \cdot \bar{V}) \bar{V} = -\nabla p + \mu \nabla^2 V + \rho \bar{f} \dots\dots\dots(26)$$

The blood density is set as $\rho = 1060 \left[\frac{kg}{m^3} \right]$, and the dynamic viscosity is $\mu = 0.004$ [pa.s].

Chapter IV

Results and Discussion

The flow and pressure characteristics for the baseline model as well as the IJS model are presented in this section. The baseline model represents the physiological flow and pressure values for the failing Fontan procedure. The cardiac output is set at an average flow of 1.2 L/min. The ratio of the flow moving through the lower circulation is maintained at 69 percent of the total cardiac output while the ratio of the flow traveling through the upper circulation is kept at 31 percent of the total cardiac output. The ratio of the flow in the pulmonary arteries is maintained at 50 percent each. The ratio of the pulmonary flow to the systemic flow (Q_p/Q_s) is one. The inferior vena cava pressure is equivalent to the failing Fontan operation. The superior vena cava pressure is roughly analogous to the pressure of the inferior vena cava. The pressure at the pulmonary arteries is similar.

The IJS model replicates the palliative technique used in this research. The flow split ratio between the upper and lower circulations is preserved. The flow split ratio between the pulmonary arteries is also maintained. The cardiac output increases to 1.77 L/min. The ratio of the pulmonary flow to the systemic flow (Q_p/Q_s) increases to (1.32). The increase in the pulmonary flow to the systemic flow ratio decreases the inferior vena cava pressure by 0.95 mmHg with respect to the baseline model. The pressure at the upper circulation decreases while the pressure at the pulmonary arteries increases. The summary of the results are shown below.

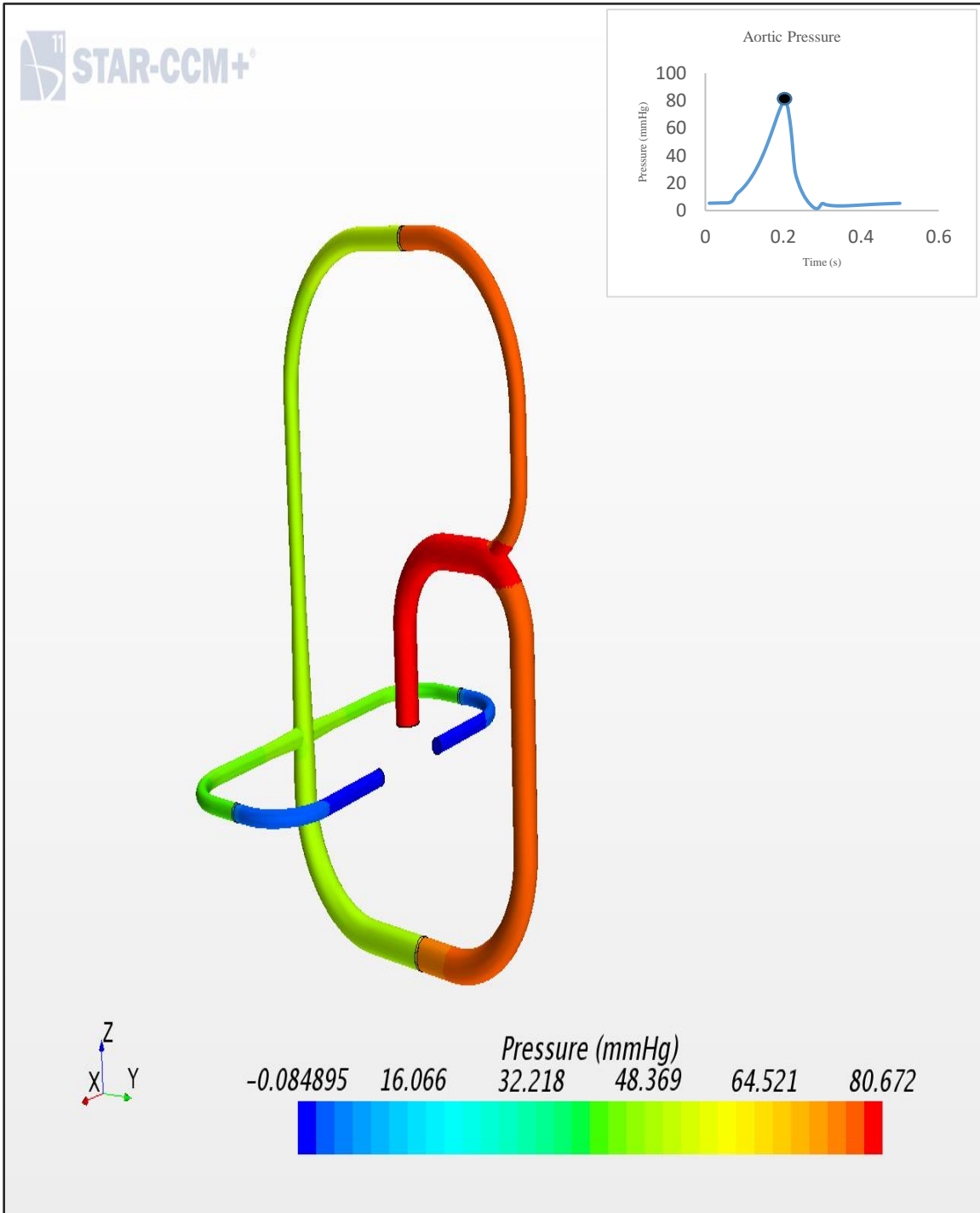


Figure 13: The baseline model pressure

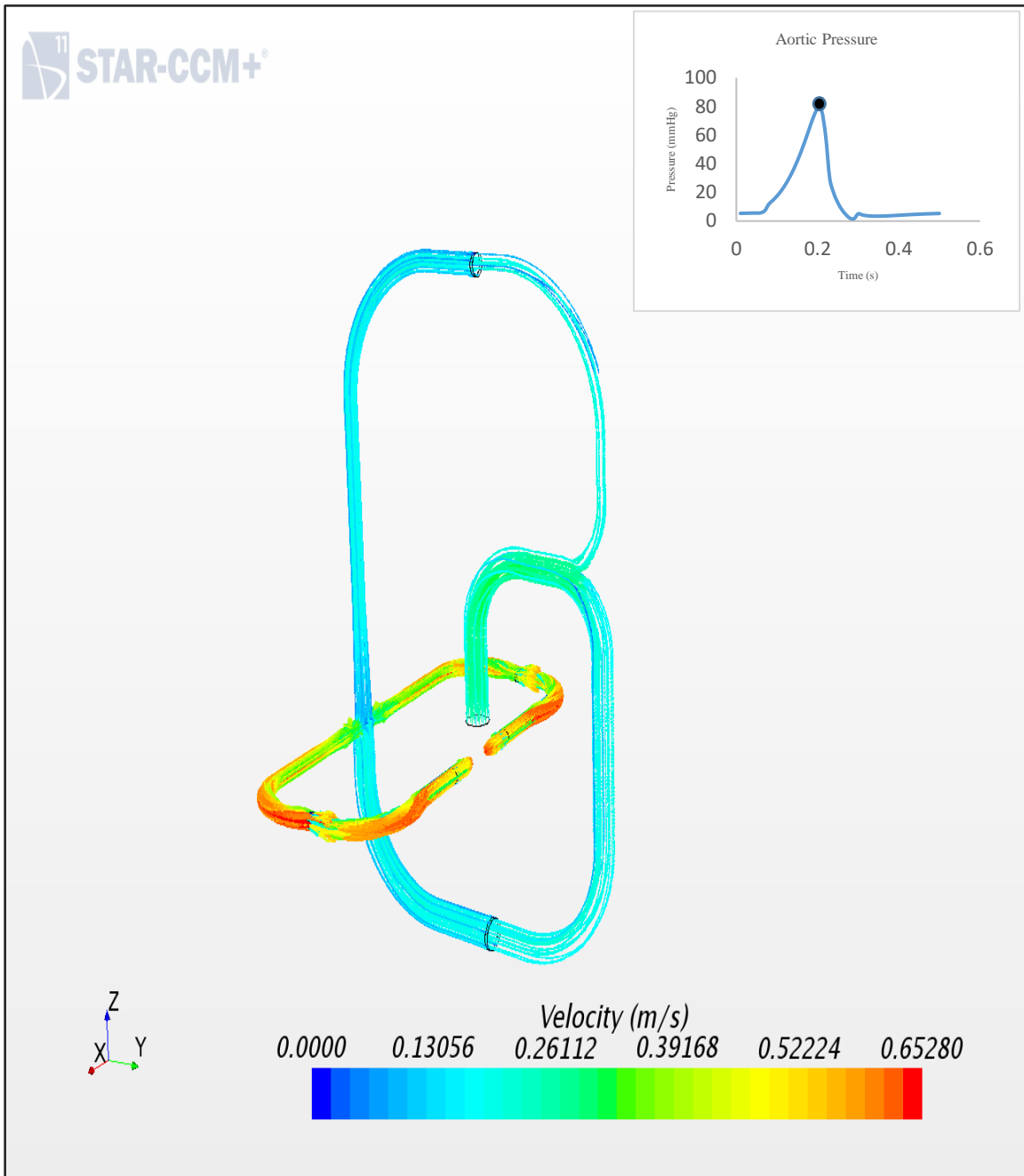


Figure 14: Velocity field of the baseline model

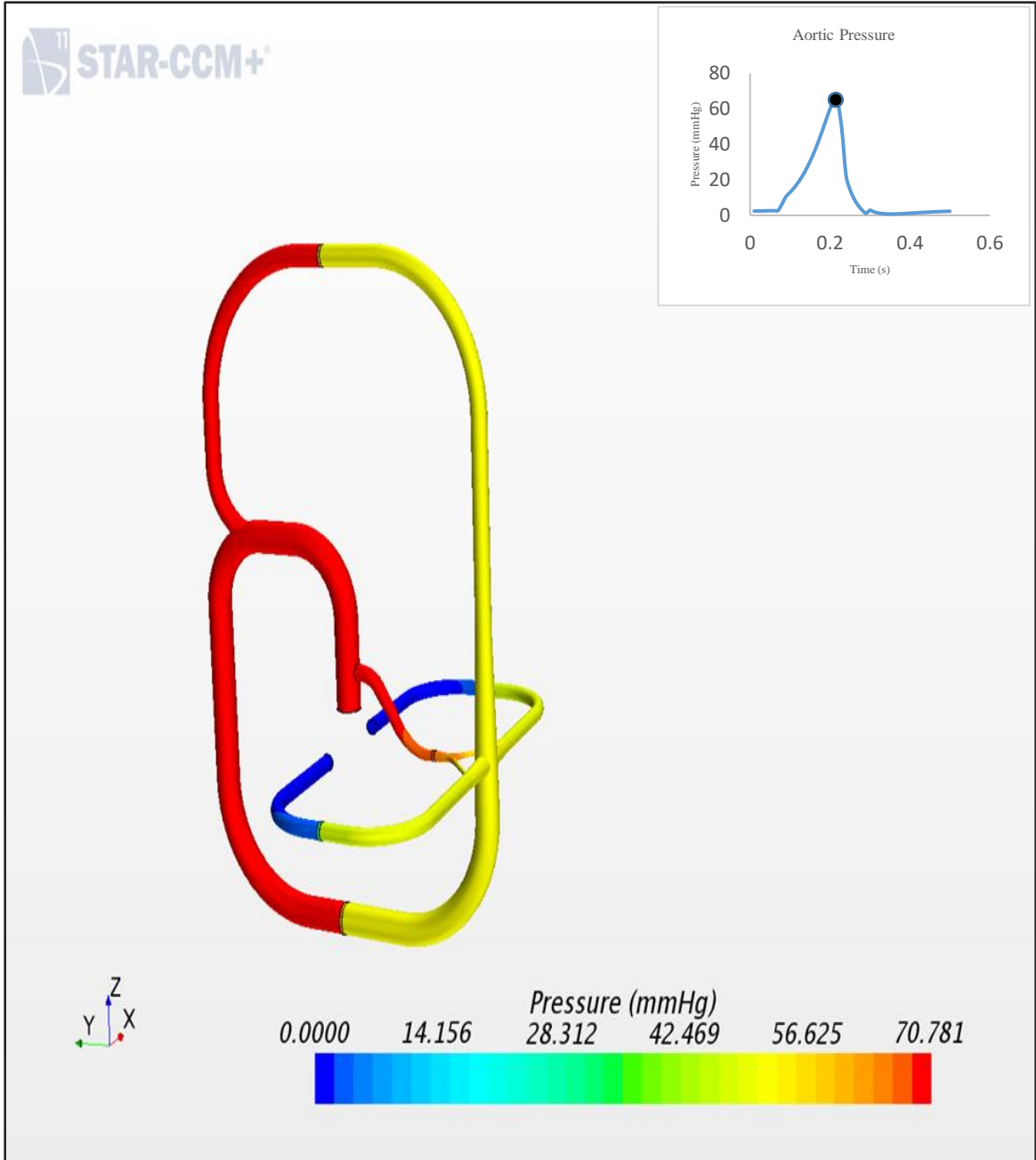


Figure 15: The IJS model pressure

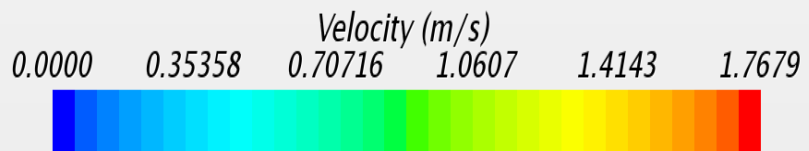
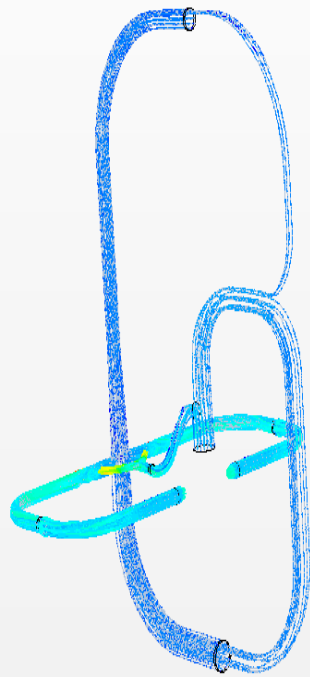
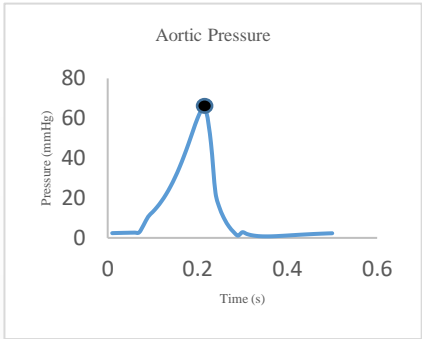


Figure 16: Velocity field of the IJS model

	Baseline	IJS
Cardiac Output (ml/s)	20	29.53
Qu / Qs (%)	31	30.8
Ql / Qs (%)	69	69.2
Qlpa / Qp (%)	50	50.01
Qrpa / Qp (%)	50	49.99
Qp /Qs	1	1.32
Qsvc (ml/s)	6.2	6.88
Qivc (ml/s)	13.8	15.46
Qlpa (ml/s)	10	14.77
Qrpa (ml/s)	10	14.76
Qijs (ml /s)	N/A	6.88

Table 1: Flow values in the baseline & IJS models

	Baseline	IJS
Pao (mmHg)	31.2	29.7
Pivc (mmHg)	23.5	22.55
P svc (mmHg)	23.2	22.1
Prpa (mmHg)	13.5	14.03
Plpa (mmHg)	13.5	14.03

Table 2: Pressure values in the baseline & IJS models

Chapter V

Conclusion – Limitation – Future Work

This research displays the Fontan Procedure baseline model as well as the IJS model. Catia V5 software was used to model the geometry incorporated in the CFD simulation in STAR CCM+ which is the second software used in this research. Furthermore, the solution generated by Lumped Parameter Model (LPM) is coupled to STAR CCM results in order to have time averaged solution that represents the convergence between the CFD and LPM. The coupling process also does eliminate the deviation between the results coming out of the CFD and the solution obtained by the lumped parameter model until the convergence achieved. After all the steps are done, the baseline model shows an acceptable blood pressure in the aorta, superior vena cava, inferior vena cava, and right and left pulmonary arteries. The aim of the blood flow distribution is to be 70 percent through the lower circulation and 30 percent through the upper circulation. Also, the aim of the blood distribution is to have 50 percent in the left pulmonary artery and 50 percent in the right pulmonary artery. This approach has been accomplished successfully. Additionally, the Injection Jet Shunt (IJS) model enhances the blood flow through the pulmonary arteries. It also reduces the inferior vena cava pressure by 0.95 mmHg. The blood flow distribution is maintained through the upper circulation, lower circulation, and pulmonary arteries.

Moreover, the limitations of this research were the speed of the computers used to run the simulations and the limited time frame that was given to get this research done. To this end, it is recommended to use a compliant model which will assist reading the results coming out of the CFD more accurately. Also, testing different diameters and angles of the IJS is vital to enhance the results.

References

- [1] Mondésert B, Marcotte F, Mongeon FP, Dore A, Mercier LA, Ibrahim R, Asgar A, Miro J, Poirier N, Khairy P. "Fontan circulation: success or failure?" *Can J Cardiol.* 2013;29(7):811-20.
- [2] Ceballos, A., Osorio, R., Kassab, A., Divo, E., Argueta-Morales, I.R., and DeCampi, W., "A Multiscale Model of the Circulatory System in Infants Undergoing Hybrid Norwood Palliation," Abstract in Proc. of 2011 Coupled Problems in Science and Engineering (Coupled 2011 ECCOMAS Conf., 20-22 June, 2011, Kos, Greece), Papadrakakis, M., Onates, E., and Scheffler, B. (eds.), CMINE, Barcelona, 2011 (CD ROM).
- [3] Piran, S. (2002). Heart Failure and Ventricular Dysfunction in Patients With Single or Systemic Right Ventricles. *Circulation*, 105(10), 1189-1194. doi:10.1161/hc1002.105182.
- [4] Congenital Heart Defects (CHDs). (2016, November 08). Retrieved March 28, 2018, from <https://www.cdc.gov/ncbddd/heartdefects/hlhs.html>.
- [5] Fontan, F., & Baudet, E. (1971). Surgical repair of tricuspid atresia. *Thorax*, 26(3), 240-248. doi:10.1136/thx.26.3.240.
- [6] Gaze, D. C. (2012). *The Cardiovascular system - physiology, diagnostics and clinical implications*. Rijeka: InTech.
- [7] Balaban, R. S. (2012). Metabolic homeostasis of the heart. *The Journal of General Physiology*, 139(6), 407-414. doi:10.1085/jgp.201210783.
- [8] Opie, L. H. (2004). *Heart physiology: From cell to circulation*. Philadelphia, Pa.: Lippincott Williams & Wilkins.
- [9] Atherosclerosis. (n.d.). Retrieved March 28, 2018, from http://sphweb.bumc.bu.edu/otlt/MPH-Modules/PH/PH709_Heart/PH709_Heart2.html.
- [10] Fruitman, D. S. (2000). Hypoplastic left heart syndrome: Prognosis and management options. *Paediatrics & Child Health*, 5(4), 219-225. doi:10.1093/pch/5.4.219
- [11] Bacha, E. A. (2013). Individualized Approach in the Management of Patients With Hypoplastic Left Heart Syndrome (HLHS). *Seminars in Thoracic and Cardiovascular Surgery: Pediatric Cardiac Surgery Annual*, 16(1), 3-6. doi:10.1053/j.pcsu.2013.01.001
- [12] Tworetzky, W., Mcelhinney, D., Reddy, M., Brook, M., Hanley, F., & Silverman, N. (2001). Improved surgical outcome after fetal diagnosis of hypoplastic left heart

- syndrome. *ACC Current Journal Review*,10(5), 89. doi:10.1016/s1062-1458(01)00434-2.
- [13] Norwood, W. I. (1986). Palliation for Hypoplastic Left Heart Syndrome. *Pediatric Cardiology*,644-645. doi:10.1007/978-1-4613-8598-1_175
- [14] Barron, D. J., Kilby, M. D., Davies, B., Wright, J. G., Jones, T. J., & Brawn, W. J. (2009). Hypoplastic left heart syndrome. *The Lancet*,374(9689), 551-564. doi:10.1016/s0140-6736(09)60563-8.
- [15] Gaynor, J. W., Mahle, W. T., Cohen, M. I., Ittenbach, R. F., Decampoli, W. M., Steven, J. M., Spray, T. L. (2002). Risk factors for mortality after the Norwood procedure. *European Journal of Cardio-Thoracic Surgery*,22(1), 82-89. doi:10.1016/s1010-7940(02)00198-7.
- [16] &. (2011). Comparison of Shunt Types in the Norwood Procedure for Single-Ventricle Lesions. *Survey of Anesthesiology*, 55(3), 111-112. doi:10.1097/sa.0b013e318218e5c8.
- [17] Ceballos, A., Argueta-Morales, I. R., Divo, E., Osorio, R., Caldarone, C. A., Kassab, A. J., & Decampoli, W. M. (2012). Computational Analysis of Hybrid Norwood Circulation with Distal Aortic Arch Obstruction and Reverse Blalock-Taussig Shunt. *The Annals of Thoracic Surgery*, 94(5), 1540-1550. doi:10.1016/j.athoracsur.2012.06.043.
- [18] Sano, S., Huang, S., Kasahara, S., Yoshizumi, K., Kotani, Y., & Ishino, K. (2009). Risk Factors for Mortality After the Norwood Procedure Using Right Ventricle to Pulmonary Artery Shunt. *The Annals of Thoracic Surgery*,87(1), 178-186. doi:10.1016/j.athoracsur.2008.08.027.
- [19] HLHS Treatment. (n.d.). Retrieved March 28, 2018, from <http://www.hearts-of-hope.org/congenital-heart-disease/hlhs-treatment/stage-1-norwood>.
- [20] Talwar, S., Nair, V., Choudhary, S., & Airan, B. (2014). The Hemi-Fontan operation: A critical overview. *Annals of Pediatric Cardiology*,7(2), 120. doi:10.4103/0974-2069.132480.
- [21] Petrucci, O., Khoury, P. R., Manning, P. B., & Eghtesady, P. (2010). Outcomes of the bidirectional Glenn procedure in patients less than 3 months of age. *The Journal of Thoracic and Cardiovascular Surgery*,139(3), 562-568. doi:10.1016/j.jtcvs.2009.08.025.
- [22] HLHS Treatment. (n.d.). Retrieved March 28, 2018, from <http://www.hearts-of-hope.org/congenital-heart-disease/hlhs-treatment/stage-2-bcps>.
- [23] Ohuchi, H. (2017). Where Is the “Optimal” Fontan Hemodynamics? *Korean Circulation Journal*,47(6), 842. doi:10.4070/kcj.2017.0105.

- [24] Khairy, P., Fernandes, S. M., Mayer, J. E., Triedman, J. K., Walsh, E. P., Lock, J. E., & Landzberg, M. J. (2008). Long-Term Survival, Modes of Death, and Predictors of Mortality in Patients with Fontan Surgery. *Circulation*,117(1), 85-92. doi:10.1161/circulationaha.107.738559.
- [25] Marcelletti, C. F., Hanley, F. L., Mavroudis, C., Mcelhinney, D. B., Abella, R. F., Marianeschi, S. M., Fontan, F. (2000). Revision of previous Fontan connections to total extracardiac cavopulmonary anastomosis: A multicenter experience. *The Journal of Thoracic and Cardiovascular Surgery*,119(2), 340-346. doi:10.1016/s0022-5223(00)70190-5.
- [26] Fredenburg, T. B., Johnson, T. R., & Cohen, M. D. (2011). The Fontan Procedure: Anatomy, Complications, and Manifestations of Failure. *RadioGraphics*,31(2), 453-463. doi:10.1148/rg.312105027.
- [27] Kogon, B., Khairy, P., & Poirier, N. (2012). Is the Extracardiac Conduit the Preferred Fontan Approach for Patients With Univentricular Hearts?: The Extracardiac Conduit Is the Preferred Fontan Approach for Patients With Univentricular Hearts. *Circulation*,126(21), 2511-2515. doi:10.1161/circulationaha.111.076398.
- [28] The Fontan Procedure - Contemporary Techniques Have Improved Long-Term Outcomes. (n.d.). Retrieved March 25, 2018, from <https://www.scribd.com/document/273992144/The-Fontan-Procedure-Contemporary-Techniques-Have-Improved-Long-Term-Outcomes>.
- [29] Otto, C. M. (2016). Heartbeat: Focus on the Fontan patient. *Heart*,102(14), 1073-1074. doi:10.1136/heartjnl-2016-310114.
- [30] Pundi, K., Pundi, Kn., Cetta, F., & Li, Z. (2018). Liver Disease in the Patient with Fontan Operation. *Congenital Heart Disease*,6(3), 190-201. doi:10.1111/j.1747-0803.2011.00504.x.
- [31] Tang, E., Restrepo, M., Haggerty, C. M., Mirabella, L., Bethel, J., Whitehead, K. K., . . . Yoganathan, A. P. (2014). Geometric Characterization of Patient-Specific Total Cavopulmonary Connections and its Relationship to Hemodynamics. *JACC: Cardiovascular Imaging*,7(3), 215-224. doi:10.1016/j.jcmg.2013.12.010.
- [32] STAR-CCM+ Documentation – Version 11.02

Appendices

Appendix 1: Abbreviations Resulted from the Equations

E_{min}	Minimum elastance
E_{max}	Maximum elastance
P_{ra}	right atrium pressure
P_{rv}	right ventricle pressure
P_{ao}	aortic pressure
Q_{sca}	superior circulation artery flow
P_{sc}	superior circulation pressure
Q_{ica}	inferior circulation artery flow
P_{ic}	inferior circulation pressure
Q_{lpa}	left pulmonary artery flow
P_{lpc}	left pulmonary circulation pressure
P_{rpc}	right pulmonary circulation pressure
Q_{rpa}	right pulmonary artery flow
P_j	total cavopulmonary connection pressure

Appendix 2: The Fontan Procedure Model Parameters

No.	Parameter	Value
1	Δt	0.000001
2	Tmax	0.275
3	E _{max}	0.5
4	E _{min}	0.06
5	R_{lpv}	0.05
6	C_{ra}	4.4
7	R_{tv}	0.05
8	C_{ao}	0.08
9	L_{sca}	0.001
10	C_{sc}	2.66
11	R_{svc}	0.9
12	L_{ica}	0.001
13	R_{ica}	2.66
14	C_{ic}	2.66
15	R_{ivc}	0.4
16	L_{lpa}	0.001
17	C_{lpc}	2.66
18	L_{rpa}	0.001
19	R_{rpa}	0.1
20	C_{rpc}	2.66
21	R_{rpv}	2.66
22	R_{lpa}	0.1
23	R_{sca}	3.25
24	R_{pv}	0.05
25	C_j	0.1

Appendix 3: Modeling Instructions

From the **file** menu, select **New Simulation**.

In the Create New Simulation window, click **Parallel on Local Host**.

Select how many nodes needed to run parallel simulation on the local machine

Click **Ok**

The simulation tree will appear.

A. 3D CAD Model Import:

In the **Geometry tree**, right click on **3D-CAD Models**.

Click **New**

Right Click on **3D-Cad Models**

Select **Import CAD Model**

Open the 3D-CAD model prepared to the simulation.

The 3D-CAD model is uploaded

Click **Update 3D-CAD**

Click **Close 3D-CAD**

Under the **3D-CAD Models** tree, right click on **3D-CAD Model 1**

Click **New Geometry Part**

Click **OK** on **Part Creation Options**

Open **Parts** tree

Right click on **Body 1**

Select **Repair CAD**

Change **Faces to show on Start Up** to **All Faces** in the drop down list

Click **Ok**

Click **Execute**

If errors appear, click **Auto-Repair Geometry Errors**

Click **Close**

Open **Body 1** tree

Open **Surfaces** tree

Right click on **Default**

Select **Split by Angle**

Change the angle to the suitable angle to split the model

Click **Ok**

Right click on **Body 1**

Click **Assign Parts to Regions**

Select **Body 1**

Change **Create One Region for All Parts** to **Create a Region for Each Part**

Change **Create a Boundary for Each Part** to **Create a Boundary for Each**

Par Surface

Click **Apply**

B. Mesh:

Right click on **Operations**

Select **New**

Select **Automated Mesh**

Click **Parts**

Click **Surface Remesher**

Click **Automatic Surface Repair**

Select **Polyhedral Mesher**

Select **Thin Mesher**

Select **Prism Layer Mesher**

Click **Ok**

Open **Automated Mesh** tree

Open **Default Controls** tree

Click **Base Size**

Set base size value

Right click on **Automated Mesh**

Select **Execute**

From the mesh menu, select **Diagnostics**

Check the validity of the mesh. Any negative volumes make the mesh invalid.

C. Physics Setup:

Right click on **Continua**

Select **New**

Select **Physics continuum**

Right click on **Physics 1**

Click **Select Models**

Under **Space**, Select **Three Dimensional**

Under **Time**, Select **Implicit Unsteady**

Under **Material**, select **Liquid**

Under **Flow**, select **Segregated Flow**

Under **Equation of State**, select **Constant Density**

Under **Viscous Regime**, select **Laminar**

Click **close**

Open **Models** tree

Open **Liquid** tree

Right click **Rename**

Change Liquid name to Blood

Open **Blood** tree

Open **Material Properties** tree

Open **Density** tree

Click **Constant**

Set density value

Open **Dynamic Viscosity** tree

Click **constant**

Set Dynamic viscosity value

D. Setting Boundary conditions:

Open **tool** tree

Right click on **Tables**

Select **New Table**

Select **File Table**

Upload the table having the boundary conditions data

Open **Regions** tree

Open **Body 1** tree

Open **Boundaries** tree

Right click on **Default**

Click **Edit**

Under **Type**, change the boundary condition type for both inlets and outlets from the drop down list.

Open **Physics Values** tree

Select table name from the drop down list

Select table data from the drop down list

Click **Close**

E. Setting Reports:

Right click on **Derived Parts**

Select **New Part**

Select **Section**

Select **Constrained Plane**

Set the locations needed to take reports from

Click **Create**

Right click on **Reports**

Select **New Report**

Select the desired field report

Right click on the selected report

Click **Edit**

Under **parts**, select the constrained plane created in the previous step

F. Setting Plots:

Right click on the selected report

Click **Create Monitor and Plot from Report**

Select **Single Plot** to create one single plot file

G. Setting Streamline:

Right click on **Derived Parts**

Select **New Part**

Select **Streamline**

Under **Seed Parts**, select **Regions**

Click **Ok**

Select **Create**

H. Scene Creation:

H.1 Scalar Scene:

Right click on **Scenes**

Select **Scalar**

Open **Scalar 1** tree

Open **Displayer** tree

Open **Outline 1** tree

Right click on **Parts**

Select **Edit**

Open **Regions** tree

Select **Body 1**

Click **Ok**

Open **Scalar 1**

Right click on **Parts**

Select **Edit**

Open **Regions** tree

Select **Body 1**

Click **Ok**

Right click on **Scalar Field**

Select **Edit**

Under **Function**, select the scalar field

Click **Close**

H.2 Vector Scene:

Right click on **Scenes**

Select **Vector**

Open **Vector 1** tree

Open **Displayer** tree

Open **Outline 1** tree

Right click on **Parts**

Select **Edit**

Open **Regions** tree

Select **Body 1**

Click **Ok**

Open **Vector 1**

Right click on **Parts**

Select **Edit**

Open **Regions** tree

Select **Body 1**

Click **Ok**

Right click on **Vector Field**

Select **Edit**

Under **Function**, select the Vector field

Click **Close**

I. Solver Setting

Open **Solvers** tree

Click **Implicit Unsteady**

Set the time step size

Click **Close**

Open **Stopping Criteria**

Select **Maximum Inner Iterations**

Set the number of iterations per time step

Select **Maximum Physical Time**

Set the time needed to obtain a stable solution

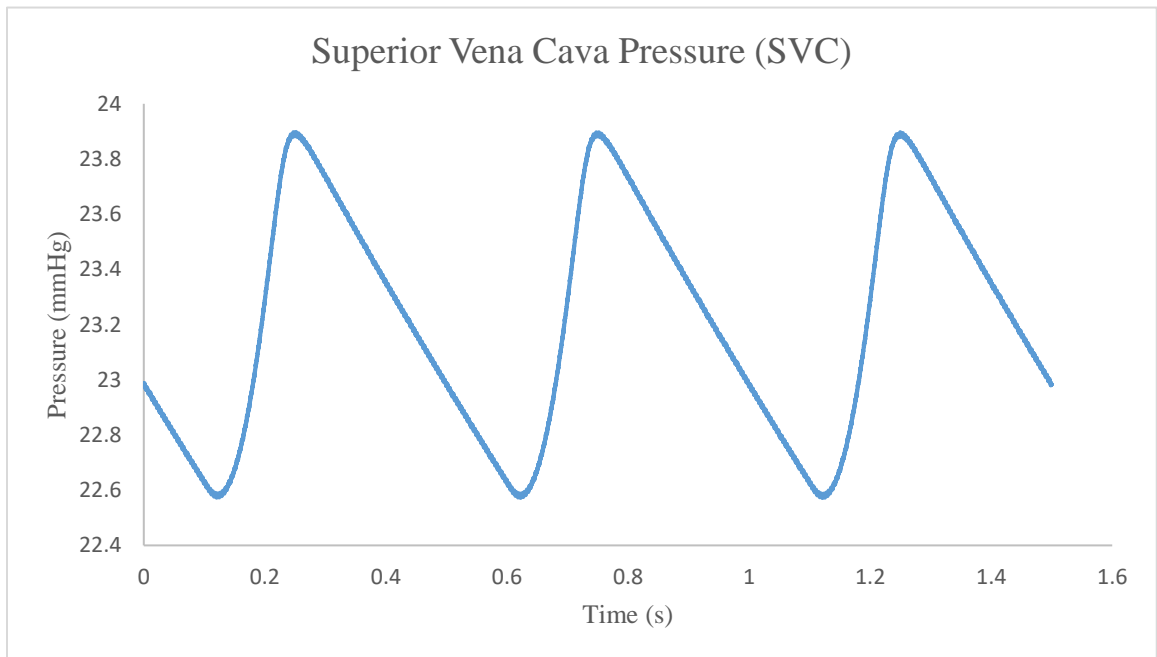
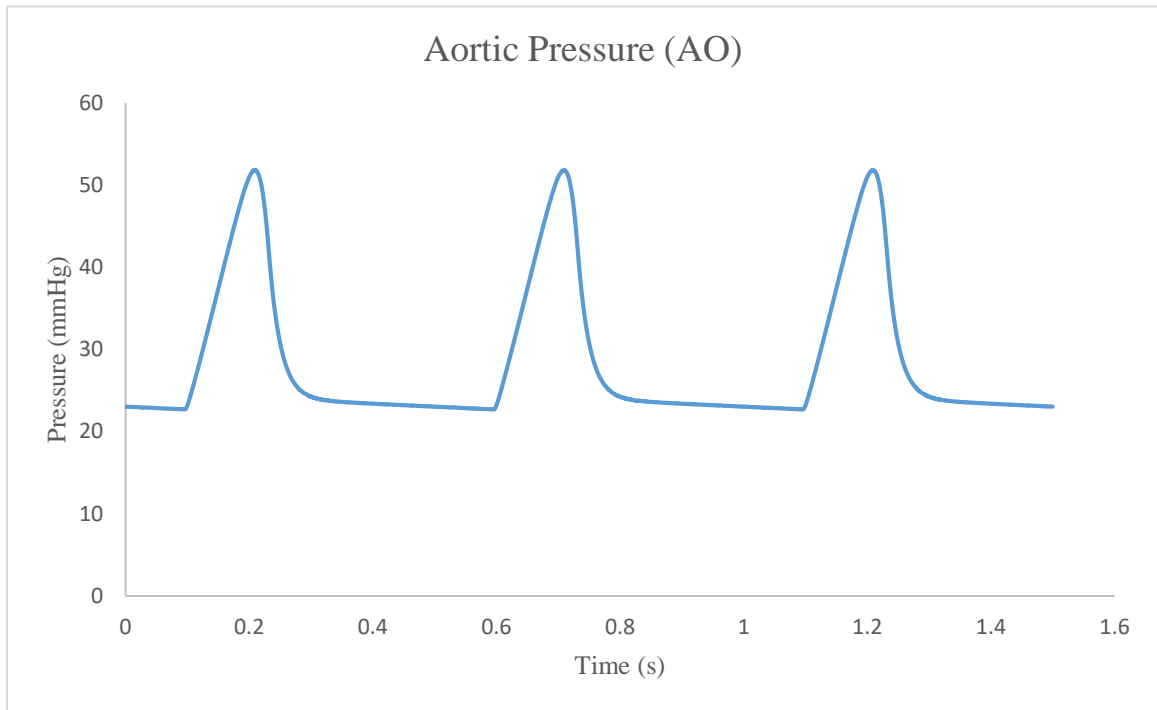
Select **Maximum Steps**

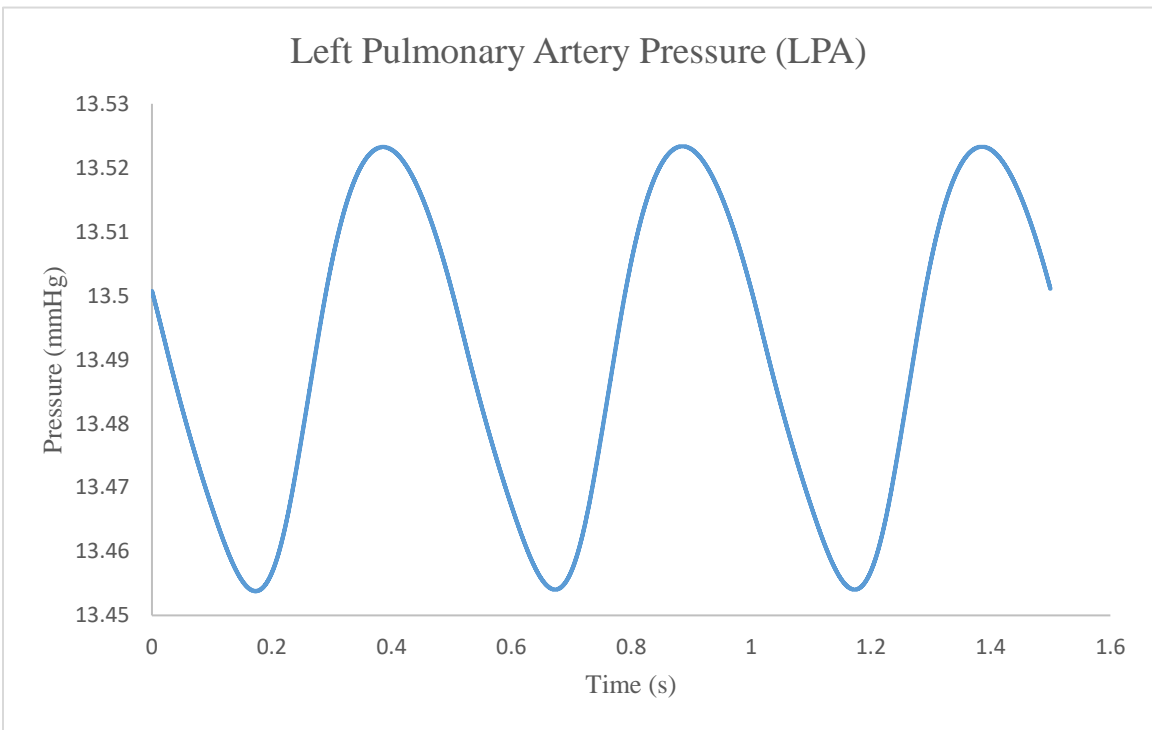
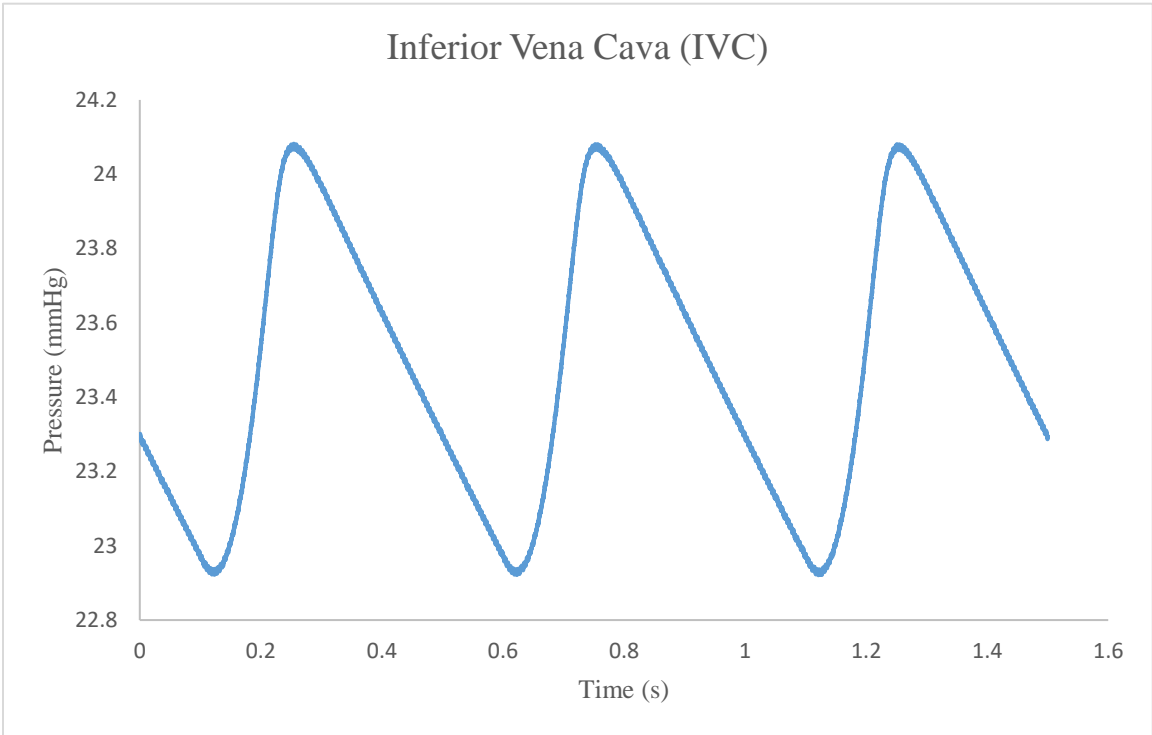
Disable the maximum steps

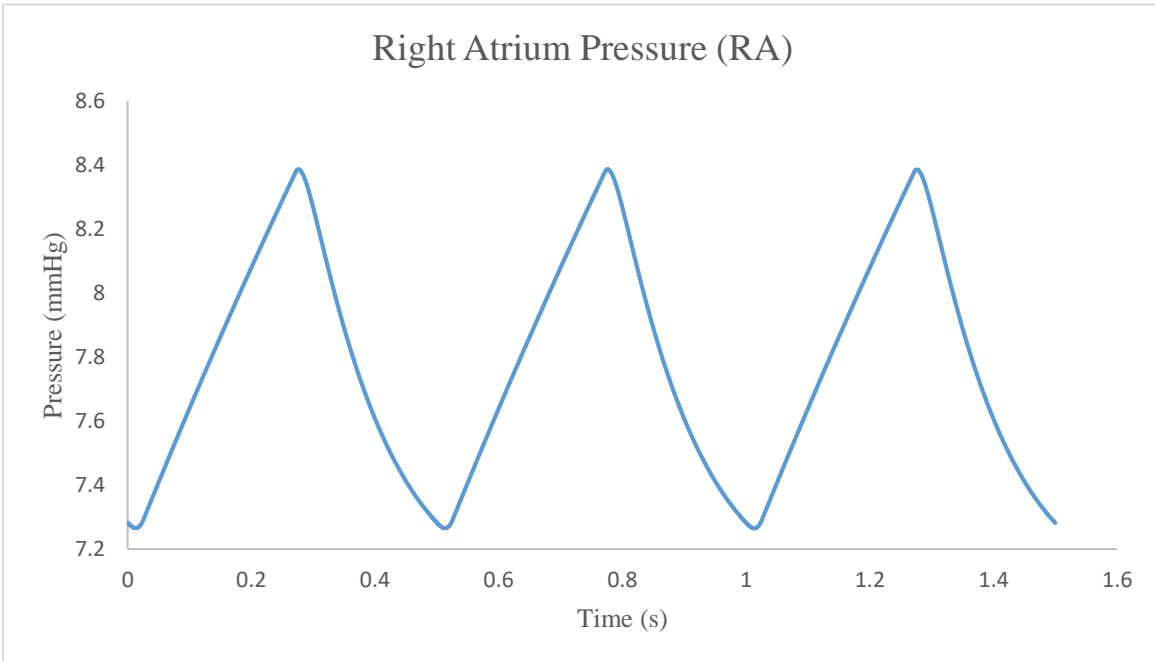
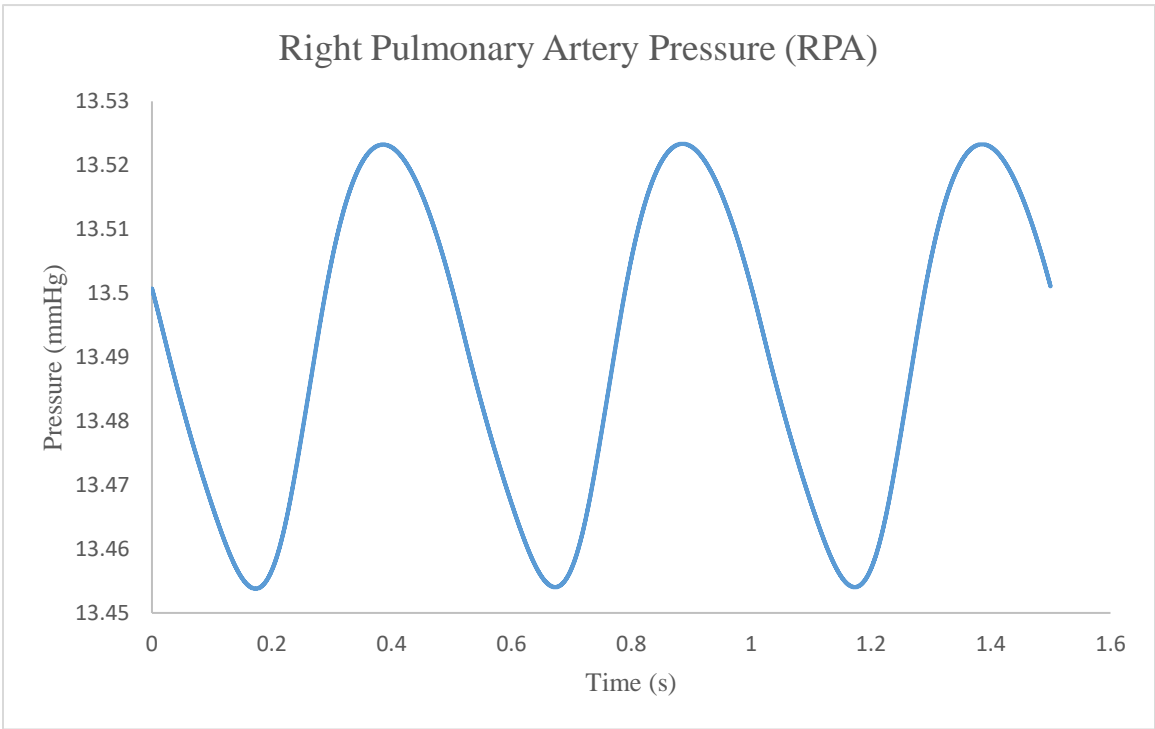
From the Solution menu, select Initialize Solution

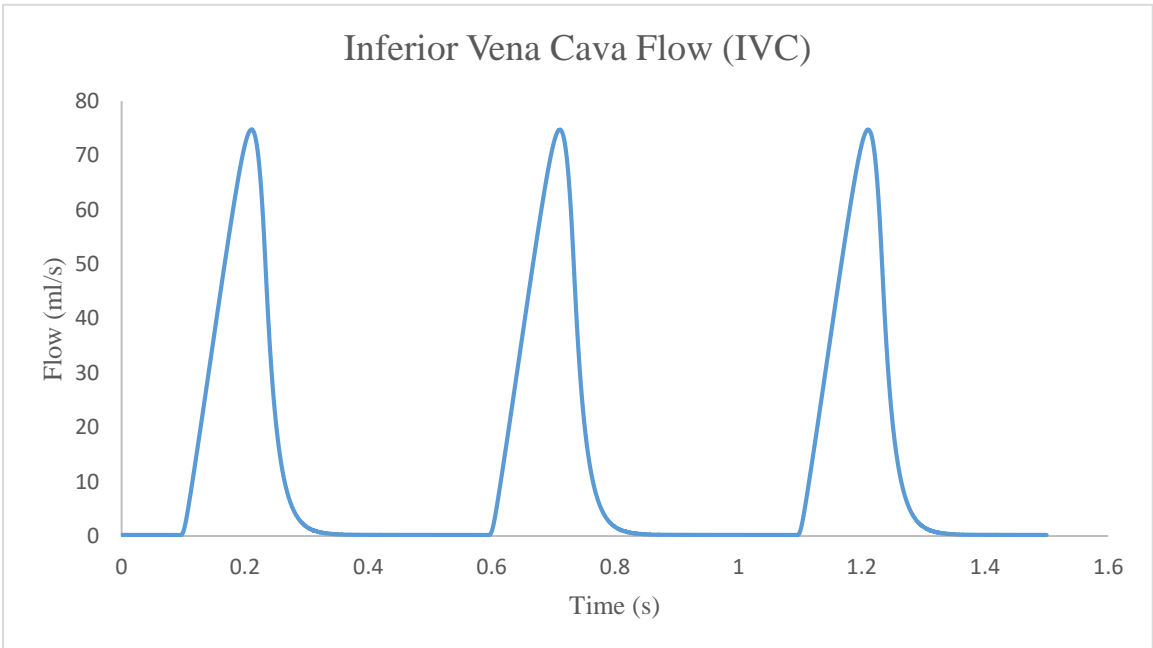
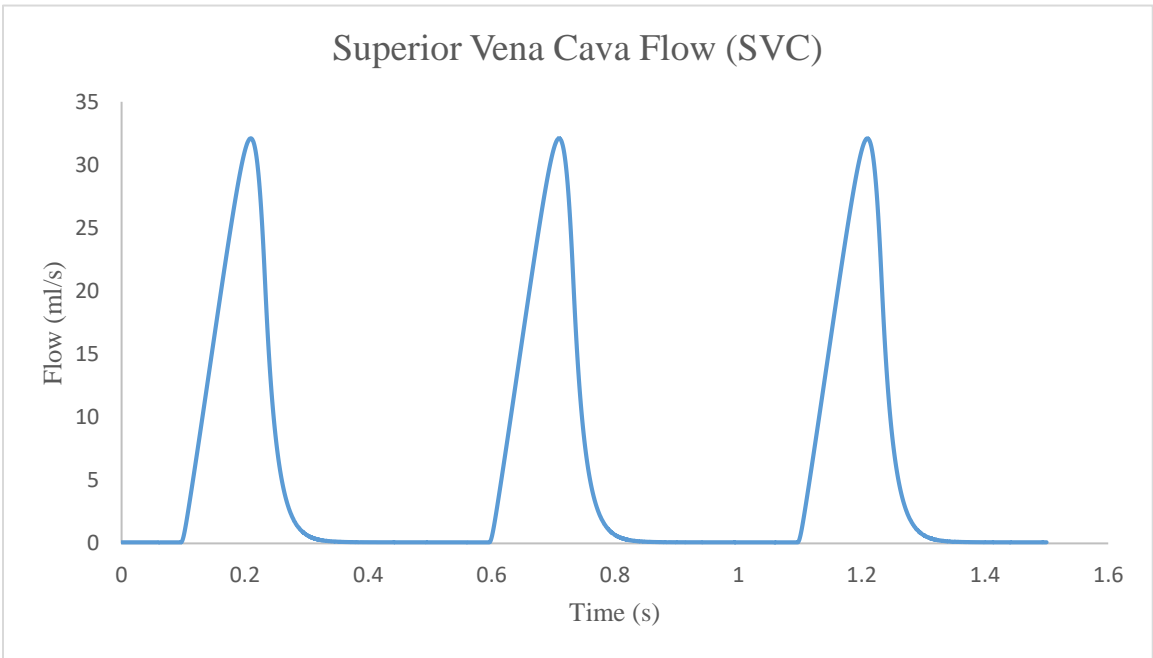
The solution is initialized and ready to run.

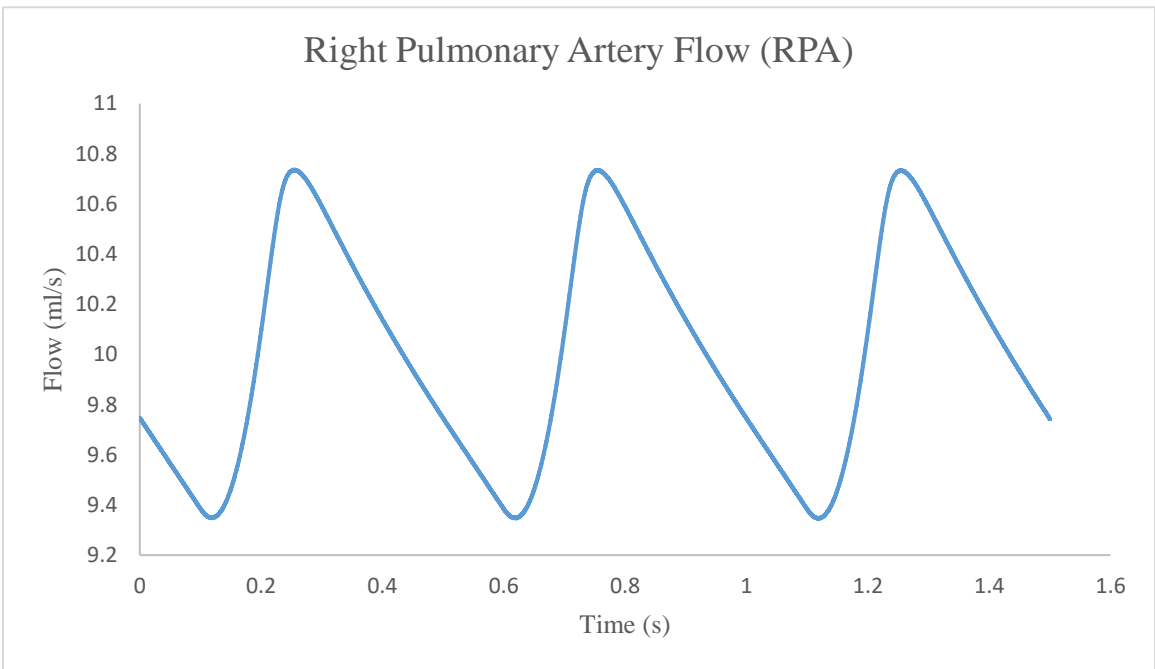
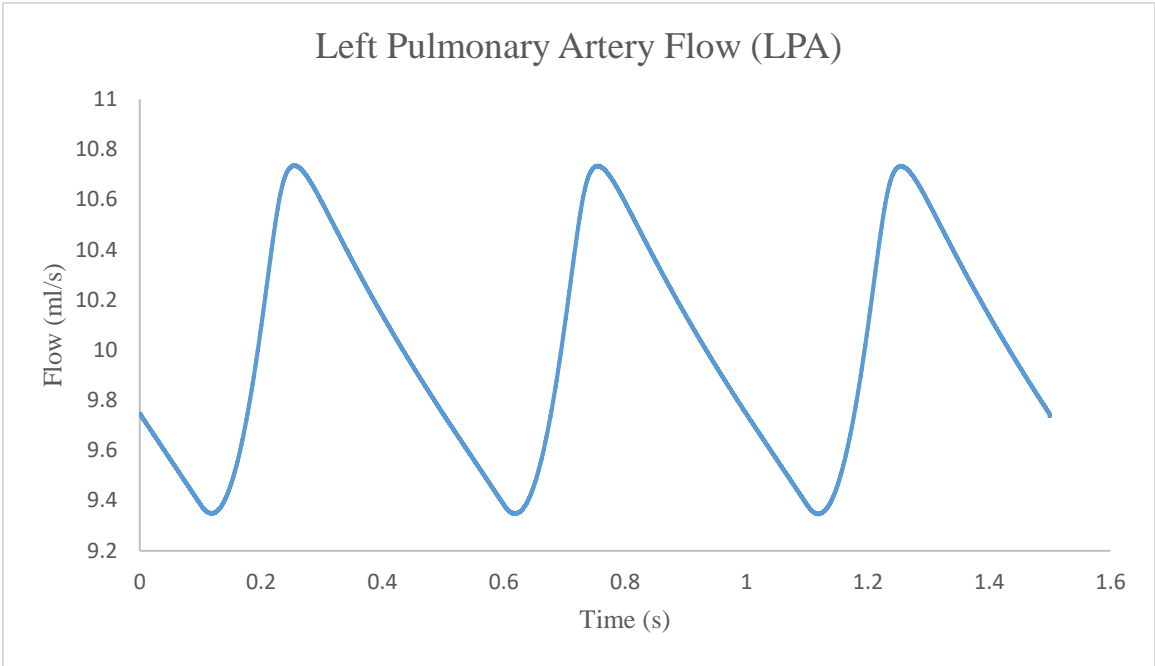
Appendix 4: CFD-LPM Coupling Charts-Baseline Model



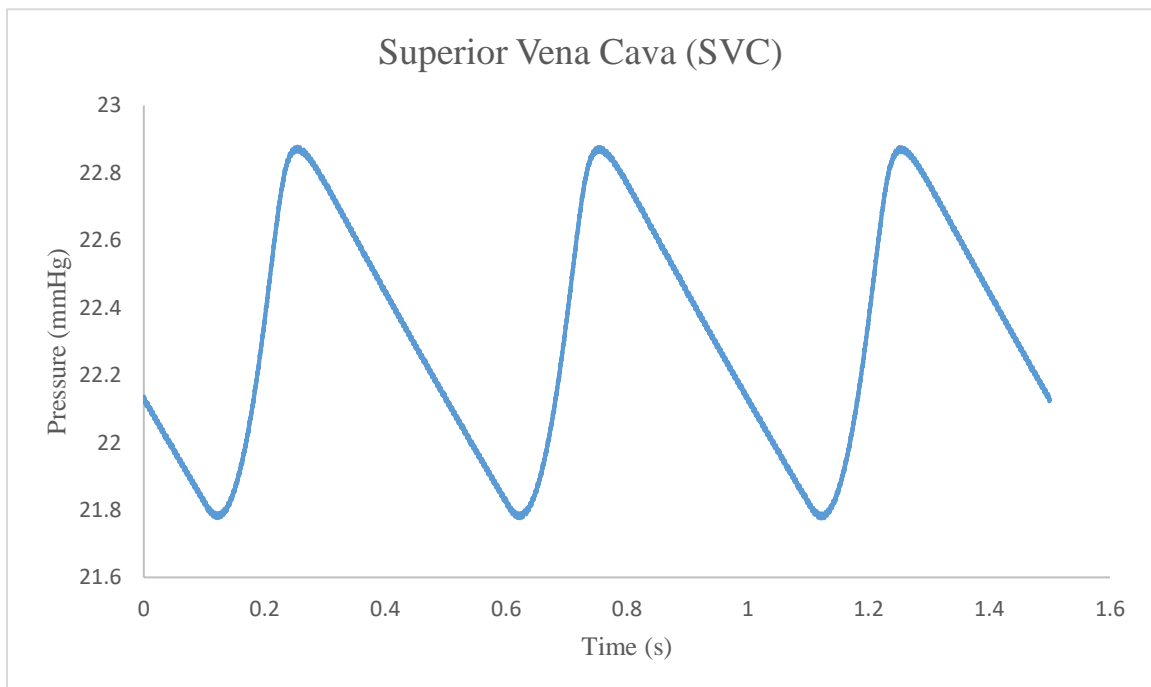
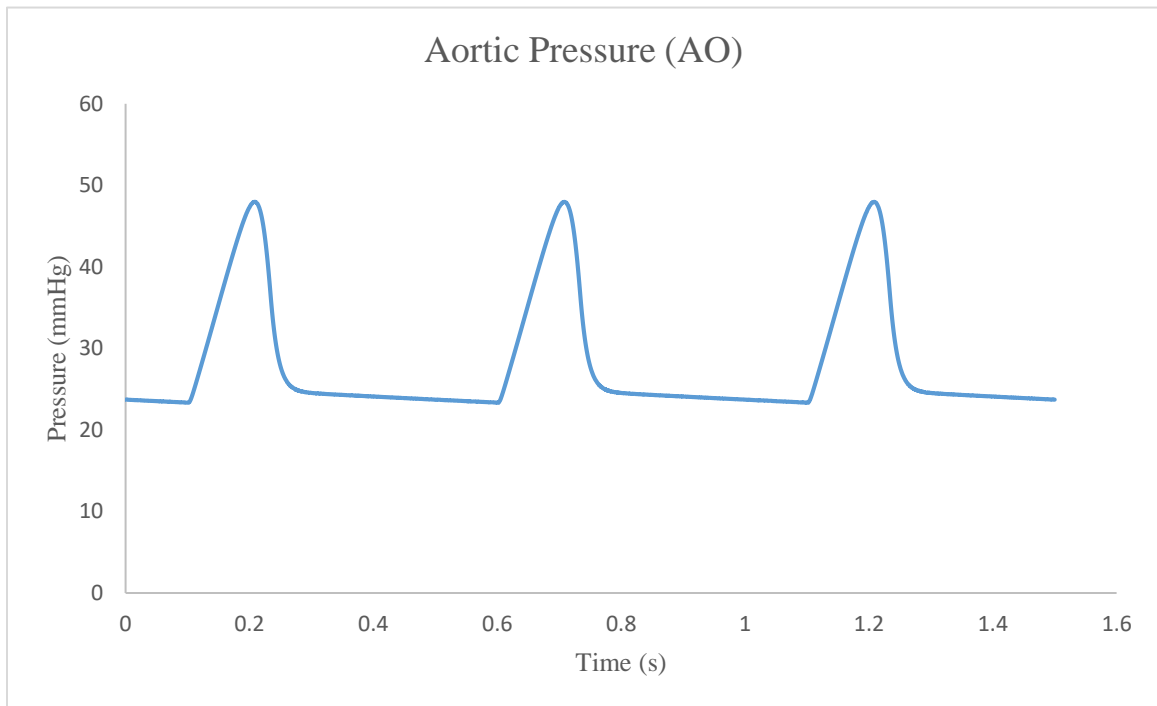


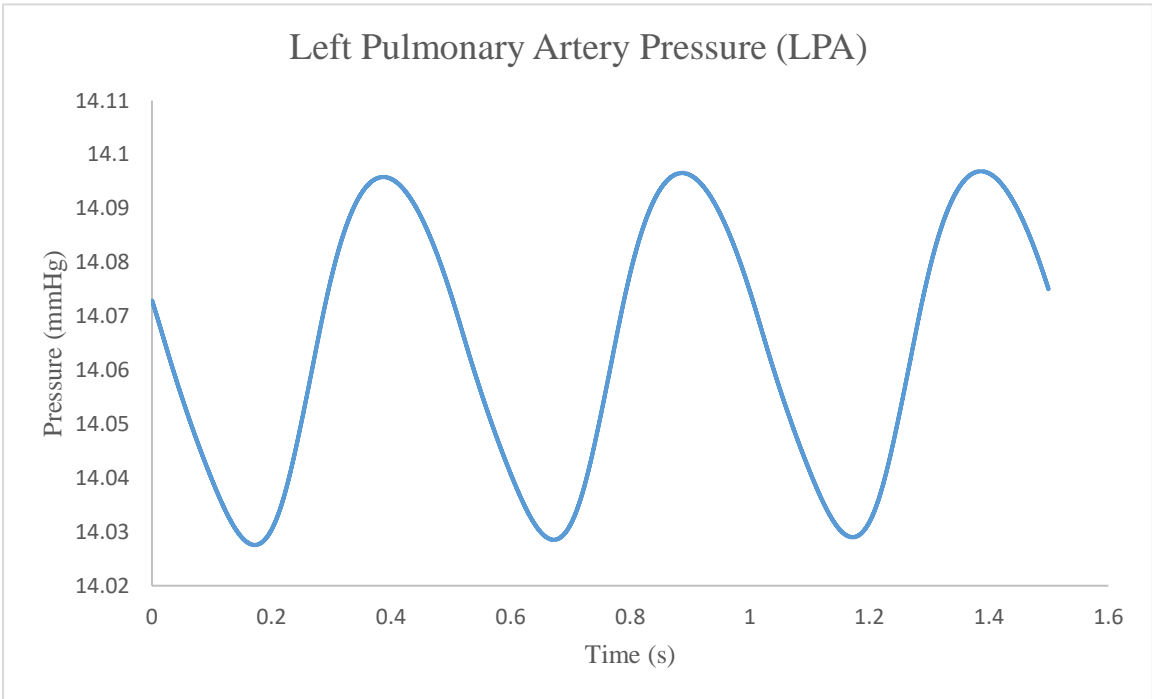
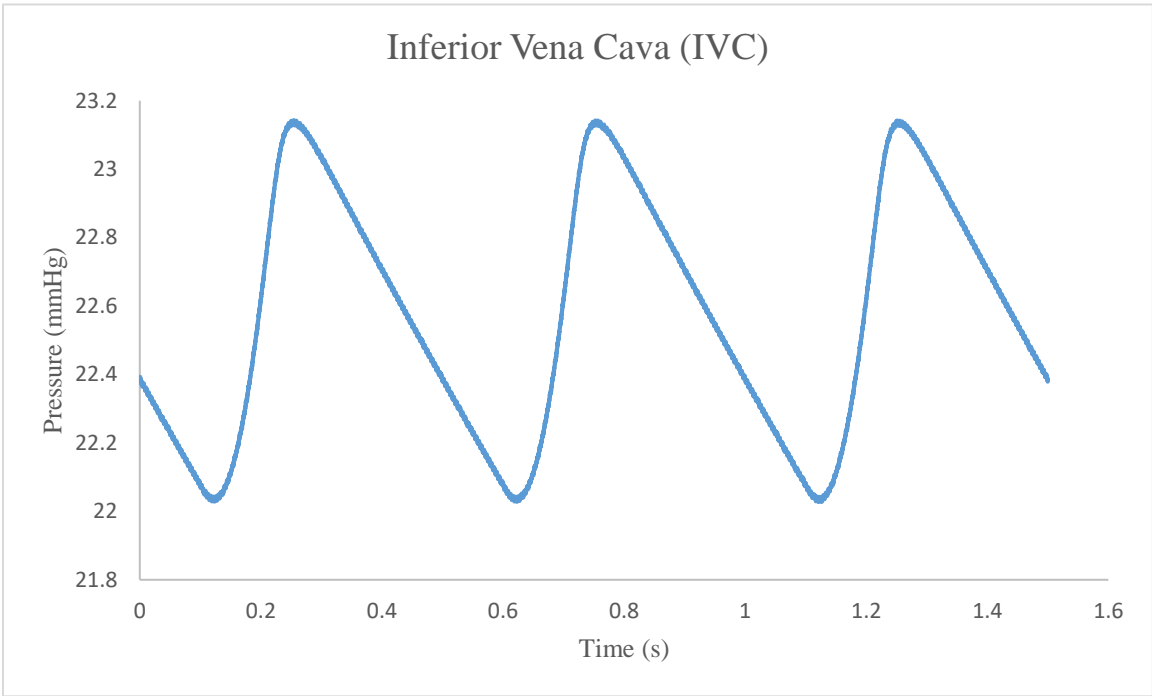


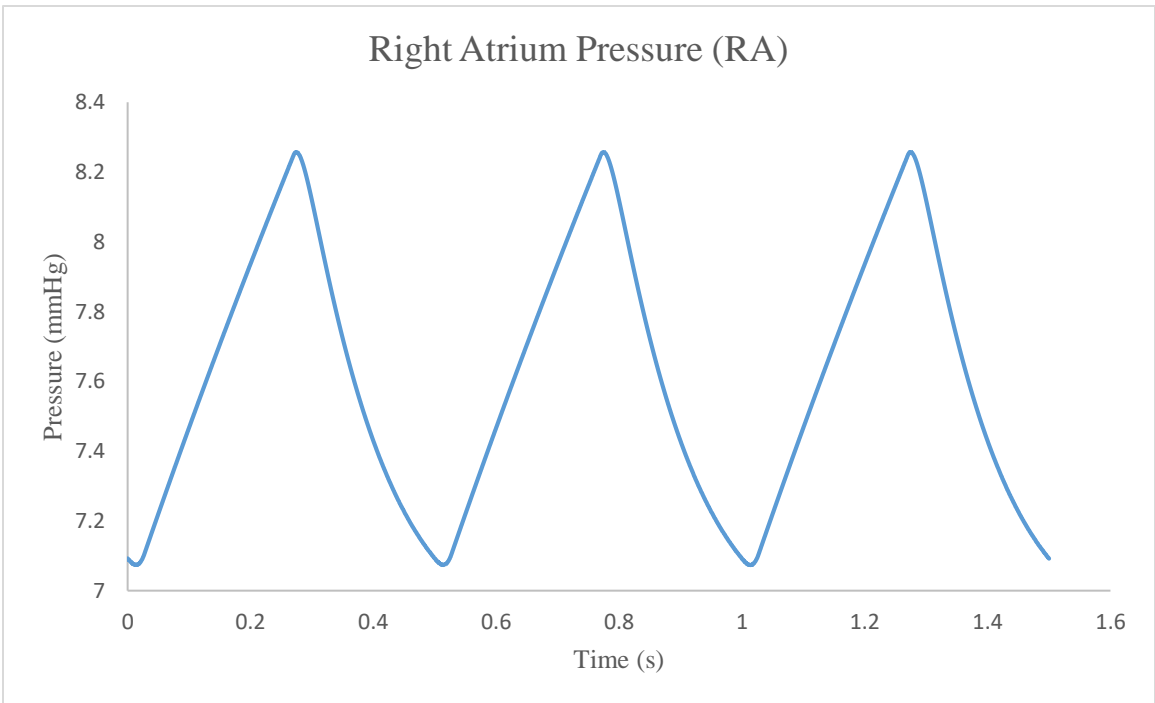
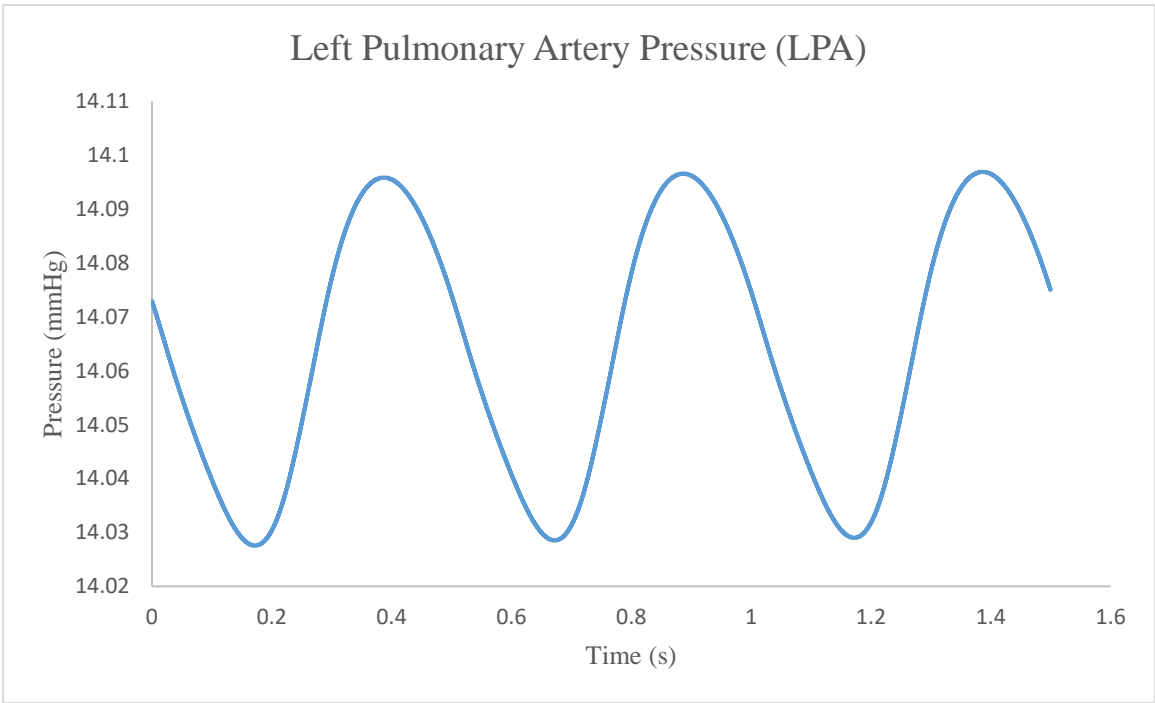


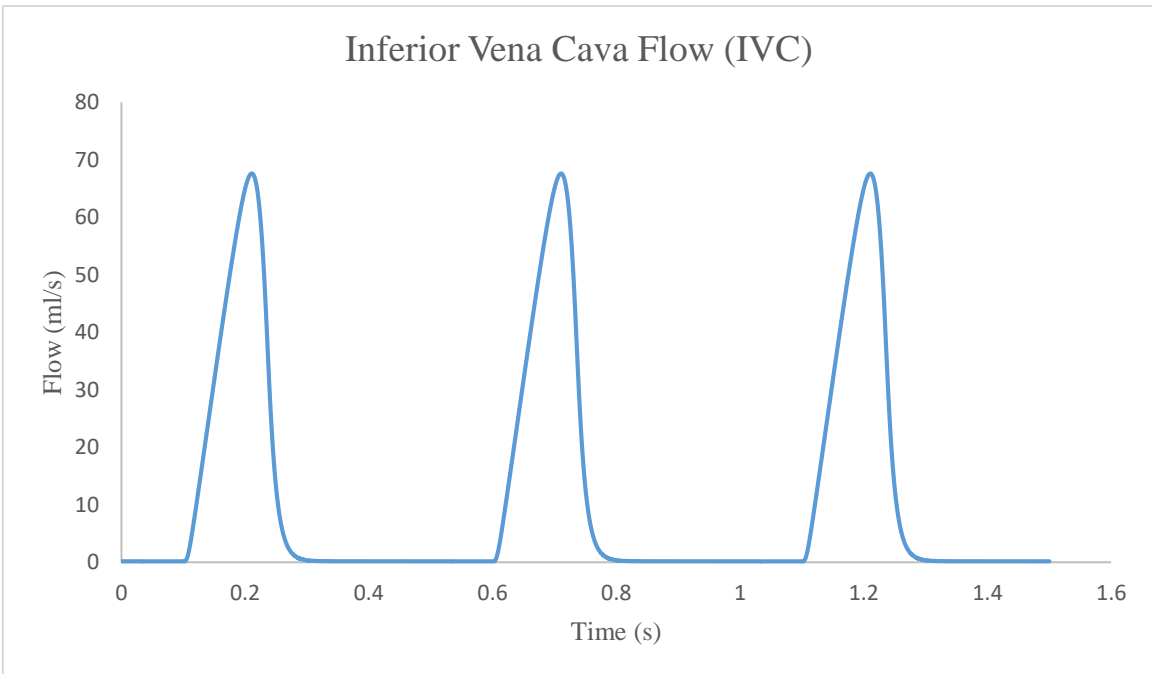
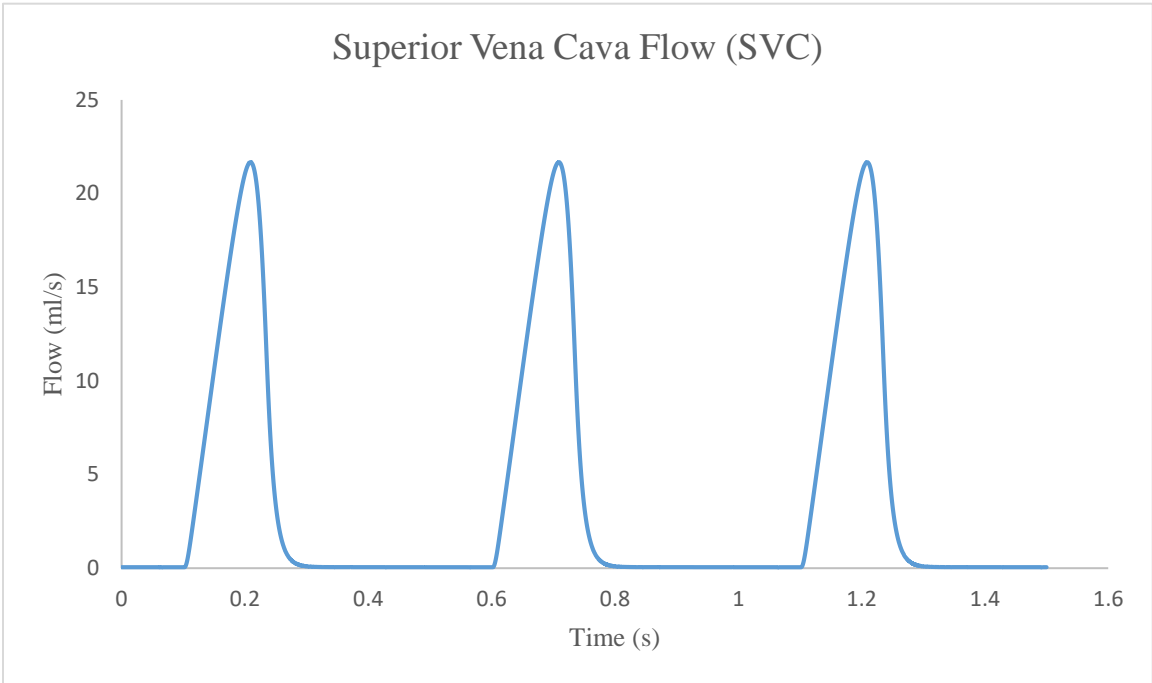


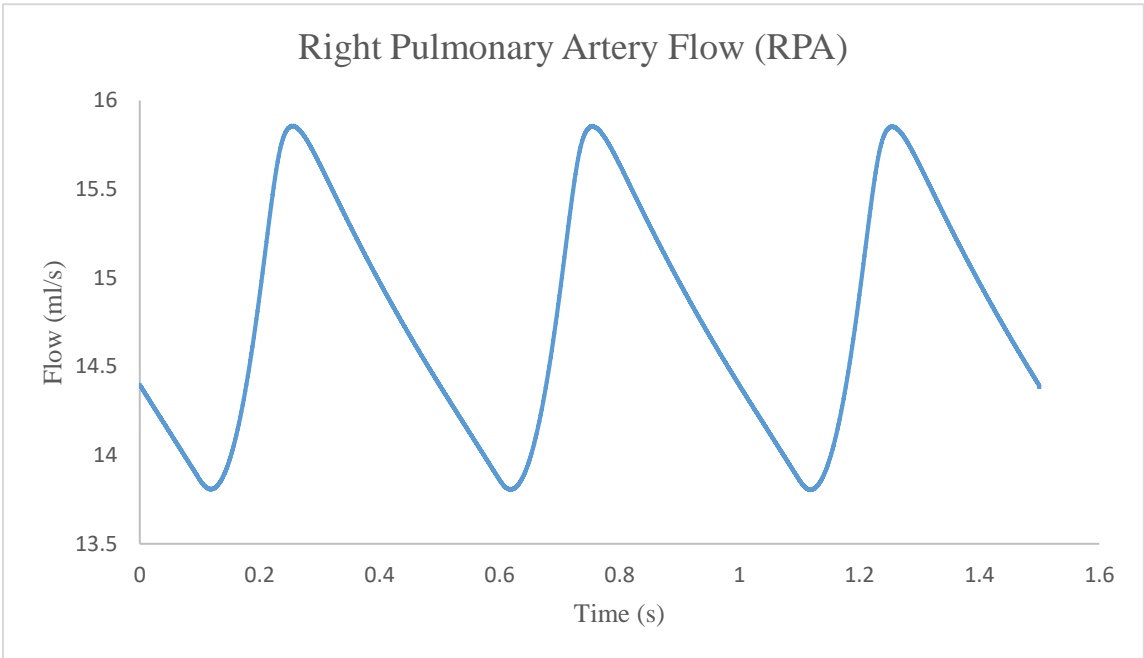
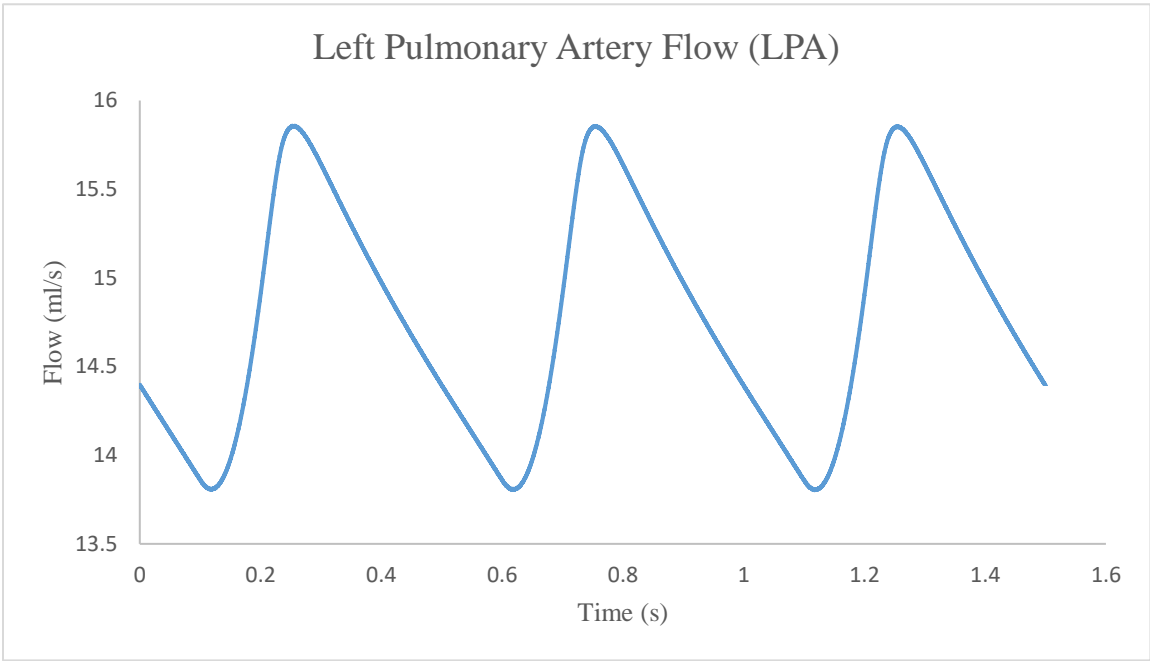
Appendix 5: CFD-LPM Coupling Charts-IJS Model

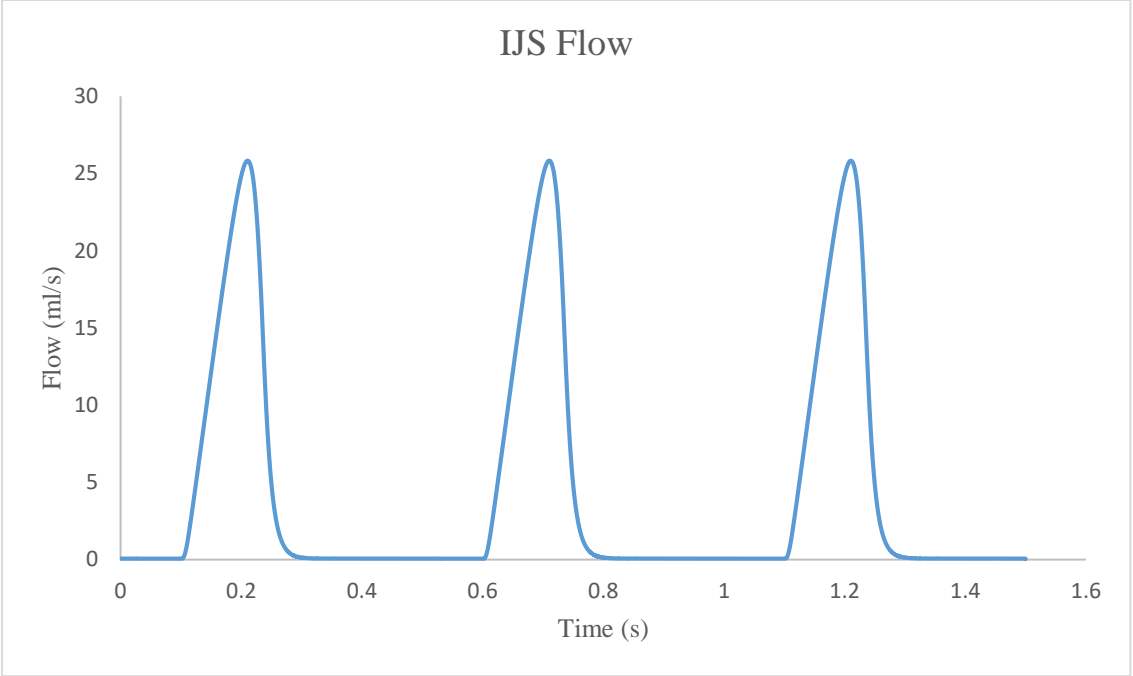




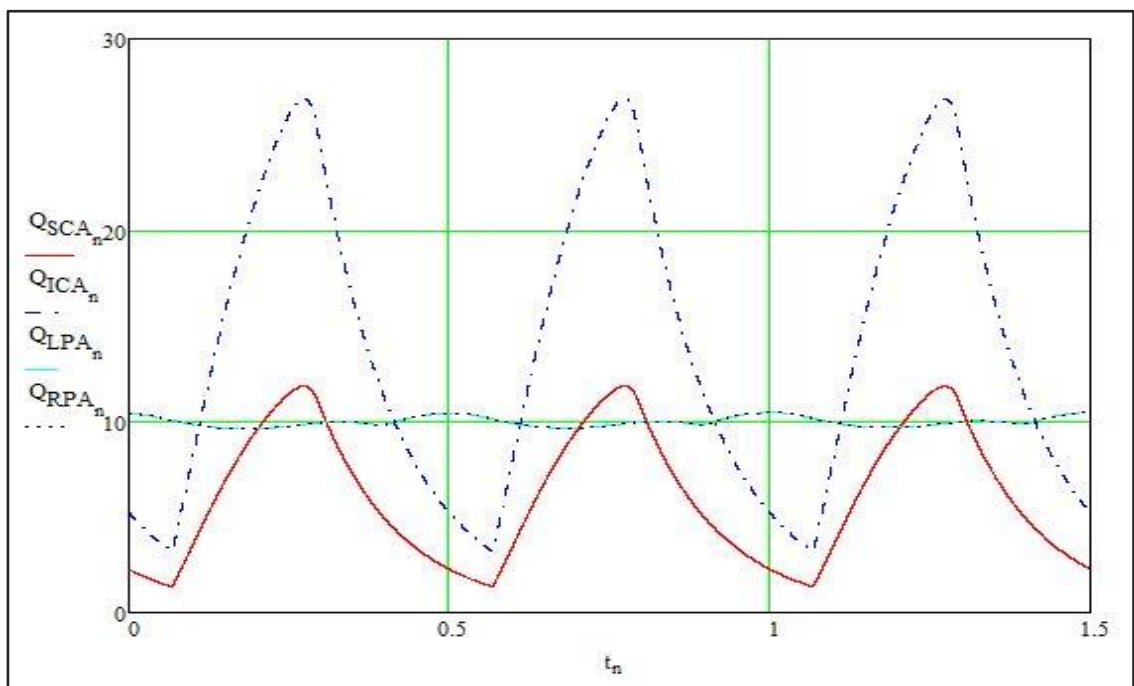
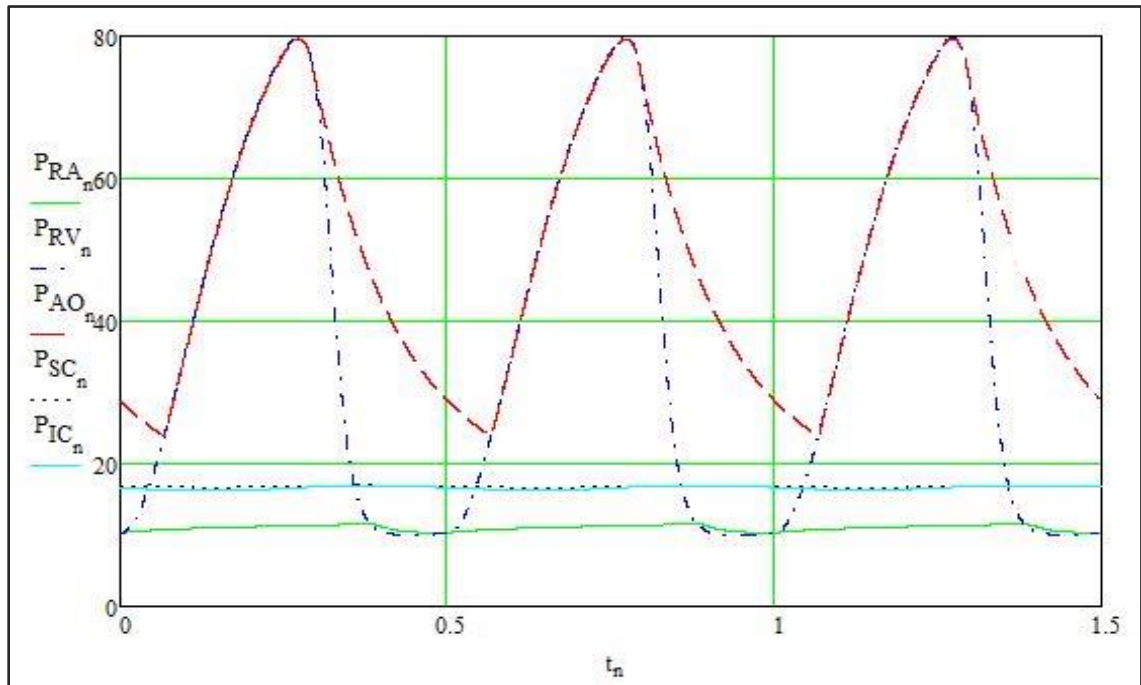








Appendix 6: LPM Pressure & Flow Charts - Baseline Model



Appendix 7: LPM Pressure & Flow Charts - IJS Model

